Original Article

AKR1C1 overexpression leads to lenvatinib resistance in hepatocellular carcinoma

Cheng Gao[1#], Liang Chang[1#], Tianxin Xu[1#], Xiaojun Li[1], Zhong Chen[2]

[1]Department of General Surgery, Affiliated Hospital of Nantong University, Medical School of Nantong University, Nantong, China; [2]Department of General Surgery, Affiliated Hospital of Nantong University, Nantong, China

Contributions: (I) Conception and design: Z Chen, C Gao; (II) Administrative support: None; (III) Provision of study materials or patients: L Chang; (IV) Collection and assembly of data: C Gao; (V) Data analysis and interpretation: C Gao, X Li, T Xu; (VI) Manuscript writing: All authors; (VII) Final approval of manuscript: All authors.

[#]These authors contributed equally to this work.

Correspondence to: Zhong Chen, MD, PhD. Department of General Surgery, Affiliated Hospital of Nantong University, 20 Xisi Road, Nantong 226001, China. Email: chenz9806@163.com.

Background: Lenvatinib is an orally administered drug that works as a multi-targeted tyrosine kinase inhibitor. It has been approved as a first-line drug after sorafenib in hepatocellular carcinoma (HCC). However, little is currently known about its treatment, targets, and possible resistance in HCC.

Methods: The proliferation of HCC cells was evaluated using colony formation, 5-ethynyl-2'-deoxyuridine (EDU), wound healing, cell counting kit-8 (CCK-8), and xenograft tumor assays. RNA sequencing (RNA-seq) was utilized to comprehensively examine variations in highly metastatic human liver cancer cells (MHCC-97H) cells (treated with various doses of lenvatinib) at the transcriptomic level. Protein interactions and functions were predicted using Cytoscape-generated networks and Kyoto Encyclopedia of Genes and Genomes (KEGG) enrichment, while the proportions of 22 immune cell types were examined with CIBERSORT. Aldo-keto reductase family 1 member C1 (*AKR1C1*) expression was verified by quantitative real time polymerase chain reaction (qRT-PCR) or immunohistochemistry in HCC cells and liver tissues. Micro ribonucleic acid (miRNAs) were predicted using online tools and potential drugs were screened using the Genomics of Drug Sensitivity in Cancer (GDSC) database.

Results: Lenvatinib inhibited the proliferation of HCC cells. The obtained results suggested that an elevated level of *AKR1C1* expression was observed in lenvatinib-resistant (LR) cell lines and HCC tissues, whereas low *AKR1C1* expression inhibited the proliferation of HCC cells. Circulating microRNA 4644 (*miR-4644*) was predicted to serve as a promising biomarker for the early diagnosis of lenvatinib resistance. Online data analysis of LR cells showed significant differences in the immune microenvironment and drug sensitivity compared with their parental counterparts.

Conclusions: Taken together, *AKR1C1* may serve as a candidate therapeutic target for LR liver cancer patients.

Keywords: Aldo-keto reductase family 1 member C1 (*AKR1C1*); lenvatinib resistance; drug sensitivity; biomarker; hepatocellular carcinoma (HCC)

Submitted Mar 29, 2023. Accepted for publication May 23, 2023. Published online Jun 30, 2023.
doi: 10.21037/jgo-23-277
View this article at: https://dx.doi.org/10.21037/jgo-23-277

Introduction

Hepatocellular carcinoma (HCC) has a high mortality rate and has been more prevalent worldwide over the past several decades. The cancer fatality and incidence rates are both considerably greater among the Chinese population compared to those in developed nations. Surgical methods are the most common treatment for HCC, although sorafenib, lenvatinib, etc. are also frequently utilized (1). Lenvatinib, a multi-target tyrosine kinase inhibitor (TKI), has shown promising results as a new first-line option in the treatment of HCC; its increased application has provided an alternative to the use of sorafenib as the sole first-line TKI treatment for HCC, which has been the case for years. Preclinical studies have demonstrated that lenvatinib has anticancer proliferation and immunomodulatory effects (2). However, only 42.9% and 25% of HCC patients with Child-Pugh A and B respond to lenvatinib (3). Similarly to sorafenib resistance, lenvatinib therapy resistance is also becoming increasingly widespread (4,5). Additionally, the immune microenvironment has an important role in the progression and development of HCC (6), but the correlation between lenvatinib-related targets and immune checkpoints remains unclear. Given the limitations of the currently available clinicopathological biomarkers, a study suggests that molecular biomarker should be used in addition to clinicopathological marker (7). There is a limited number of molecular markers that can be used to guide lenvatinib therapy and spot early lenvatinib resistance. Finding new therapeutic targets and prognostic biomarkers will facilitate more targeted approaches for the prevention and treatment of HCC (8).

Aldo-keto reductases comprise *AKR1C1-AKR1C4* are four enzymes that catalyze nicotinamide adenine dinucleotide phosphate hydride (*NADPH*)-dependent reductions and have been implicated in biosynthesis, intermediary metabolism, and detoxification. Recent research has confirmed a significant relationship between these enzymes' expression levels and both malignant transformation and cancer therapy resistance (9). In the present study, we found that *AKR1C1* was significantly enhanced in HCC cells resistant to lenvatinib and was correlated with poor patient prognosis. According to the results of this study, *AKR1C1* contributes to the development of lenvatinib resistance in oncogenic HCC. Consequently, it may be inferred that *AKR1C1* could be used as a molecular biomarker for assessing lenvatinib sensitivity and as a potential therapeutic target for individuals with HCC. We present this article in accordance with the ARRIVE reporting checklist (available at https://jgo.amegroups.com/article/view/10.21037/jgo-23-277/rc).

Highlight box

Key findings

- An elevated level of *AKR1C1* expression was observed in lenvatinib-resistant (LR) cell lines and HCC tissues. *AKR1C1* promotes the proliferation of HCC cells. Circulating *miR-4644* was predicted to serve as a promising biomarker for the early diagnosis of lenvatinib resistance of HCC patients.

What is known and what is new?

- Lenvatinib was the first drug approved for first-line treatment of HCC after Sorafenib. Lenvatinib significantly improved the objective response rate (ORR), progression-free survival (PFS), and time to progression (TTP) when compared to sorafenib therapy. However, similarly to sorafenib resistance, lenvatinib therapy resistance is also becoming increasingly widespread.
- This study found *AKR1C1* and *miR-4644* have potential prognostic significance in the prediction of LR in HCC, and *AKR1C1* could be a promising therapeutic target for patients with LR-type HCC.

What is the implication, and what should change now?

- It is necessary to explore the molecular mechanism of *AKR1C1* to mediate the changes in LR-type HCC, and weather *AKR1C1* antagonists would elevate the therapeutic effect on these HCC patients.

Methods

Cell culture

HCC cell lines (MHCC-97H, LM3, HepG2, and Hep3B) and human normal liver cells (QSG-7701) were respectively cultured in dulbecco's minimum essential medium (DMEM) or Roswell Park Memorial Institute (RPMI)-1640 medium (Thermo Fisher Scientific, Waltham, MA, USA) containing 1% streptomycin/penicillin and 10% FBS (Fetal Bovine Serum) (Thermo Fisher Scientific). The cell cultures were grown at 37 ℃ with a continuous supply of 5% carbon dioxide (CO_2). The HCC cell lines were provided by the Cell Bank at UCAS (Chinese Academy of Sciences, China). The QSG-7701 was obtained from Beyotime (Shanghai, China). Lenvatinib (Beyotime, SF5346-10 mM) concentration was progressively increased weekly up to 10 μM. After 30 weeks of treatment, HepG2 lenvatinib-resistant (LR) cell lines (with mixed cell populations, not from a single clone) were obtained.

Colony formation assay

Treatments were applied to cells that had been seeded at a density of 1,000 per well in a six-well plate. After 2 weeks, the medium was discarded, followed by washing twice with phosphate buffered saline (PBS) to remove any remaining debris. After a 30-min methanol fixation, the clones were stained with crystal violet. After being cleaned and dried, the clones were photographed.

RNA-seq and bioinformatics analysis

The extraction of total RNA was performed using a TRIzol (Invitrogen, USA)-based technique according to the manufacturer's guidelines. RNA-seq was provided by Sangon Biotech (Shanghai) Co., Ltd. According to the manufacturer's provided guidelines, the RNA concentration was measured using the Qubit2.0 (Thermo Fisher Scientific, USA), and the integrity of the RNA and the presence of genomic contamination were both examined using an agarose gel. Sequencing was performed on an Illumina HiSeq 2500 (Illumina, USA) with paired-end 150-bp read lengths. Furthermore, mRNA clean reads were mapped using TopHat2 (Johns Hopkins University, Johns Hopkins University, USA) software to the UCSC (University of California, Santa Cruz) hg38 primary assembly genome. Transcript counts were calculated using HTSeq (High-throughput sequence analysis in Python). Read normalization, size factor estimation, and differential expression analysis were performed using the Bioconductor package DESeq2 (version 3.15) (10). The datasets used in this study were uploaded to the Gene Expression Omnibus (GEO) database (GSE214324).

Analysis of differentially expressed genes (DEGs)

The Limma package (Version 3.42.2) of R programming language was used to analyze the DEGs and visualize them using a heatmap and volcano plot with an adjusted P value of less than 0.05 in each cohort (11). Furthermore, GENEMANIA software (http://genemania.org/) was employed to generate a protein-protein interaction (PPI) network of the DEGs. The degree rank of hub genes was determined using Cytoscape (National Institute of General Medical Sciences, USA) (version 3.6.1) software, and these genes were considered for further analysis (12).

Analysis of immune infiltration

CIBERSORT is an online web portal (http://cibersortx.stanford.edu/) that uses gene expression data to estimate the abundances of individual cell types in a heterogeneous cell population (13). HCC patient data were downloaded from The Cancer Genome Atlas (TCGA) database. Furthermore, the immune response of 22 tumor-infiltrating immune cells (TIICs) was assessed using CIBERSORT to evaluate the links between different groups in HCC and to determine whether there were any correlations among the TIICs.

Kyoto Encyclopedia of Genes and Genomes (KEGG) analysis

KEGG analysis was performed using R-clusterProfiler (version 3.14.3) and the enrichplot package to identify probable signaling pathways associated with the DEGs (14). The HCC patient data used for analysis was downloaded from TCGA database. Pathways with adjusted P value of less than 0.05 were considered significant, and the complete details of significant pathways are displayed in Tables S1,S2.

qRT-PCR analysis

The extraction of total RNA was performed using a TRIzol (Invitrogen)-based technique. To obtain cDNA (complementary DNA), the extracted RNA was reverse transcribed using a RevertAid First Strand cDNA Synthesis Kit (TaKaRa, Japan). According to the established method, RT-qPCR was performed on the LightCycler 480 II (Roche, USA) using the SYBR Master Mixture (TaKaRa). β-*actin* and *U6* were used as the internal control for *AKR1C1* or *miR-4644*. The $2^{-\Delta\Delta Ct}$ method was applied for the analysis of the obtained data. The primers used in this study are listed in *Table 1*.

Transduction of AKR1C1 small interfering RNAs (siRNAs)

Two *AKR1C1* siRNAs, i.e., siRNA-*AKR1C1*#1 (CTACCTTATTCATTTTCCA) and siRNA-*AKR1C1*#2 (CCGTGGAGAAGTGTAAAGA), were designed and then synthesized. *AKR1C1* siRNA transduction was carried out using riboFECTTM CP (RiboBio, Guangzhou, China) according to the manufacturer's provided guidelines.

Table 1 The sequences of primers used in this study

Genes	Primers
AKR1C1	Forward: 5'-GGCCATCCGAAGCAAGATTG-3'
	Reverse: 5'-TCTGGTCGATGGGAATTGCA-3'
MiR-4644	5'-ACACTCCAGCTGGGTGGAGAGAGAAAAGAGA-3'
U6	Forward: 5'-CTCGCTTCGGCAGCACA-3'
	Reverse: 5'-AACGCTTCACGAATTTGCGT-3'
β-actin	Forward: 5'-GGCGGCACCACCATGTACCCT-3'
	Reverse: 5'-AGGGGCCGGACTCGTCATACT-3'

Cell proliferation assay

A cell counting kit-8 (CCK-8; Sigma-Aldrich, St. Louis, MO, USA) was employed to evaluate cellular proliferation. For each condition, the results are represented as the mean ± standard error of three different experiments. When the cells in six-well plates reached 80% confluency, three scratch wounds were induced in each well using 100 µL pipette tips. After 48 h, the wound had closed, and photos were taken at 0 and 48 h. For the EdU test, the number of cells in each group was counted and observed under a fluorescence microscope (Olympus Corporation, Japan) following the application of the Cell-LightTM EdU Apollo567 kit (Ribo) *in-vitro* according to the manufacturer's provided guidelines.

Drug sensitivity analysis

The anticancer drug dataset was downloaded from the Genomics of Drug Sensitivity in Cancer (GDSC) website, and we then used the oncoPredict package to determine whether there was a link between the IC_{50} (half maximal inhibitory concentration) values of various drugs reported with anticancer activity and the different risk groups (15). The screening of drugs was performed with a standard mean IC_{50} <1 for all liver cancer samples, which were considered to be highly effective drugs for liver cancer treatment. Furthermore, statistical analyses of drug sensitivity for these drugs in the high- and low-risk subgroups were performed to determine the various levels of response to drugs in patients in different risk groups.

Human sample and immunohistochemistry

The study was conducted in accordance with the Declaration of Helsinki (as revised in 2013). Informed consent was obtained from the patients, and this research was approved by the Ethics Committee of Affiliated Hospital of Nantong University (No. 2018-L006). The data and samples were collected from patients at the Affiliated Hospital of Nantong University. Diluted *AKR1C1* monoclonal antibodies (1:400, SANTA CRUZ BIOTECHNOLOGY, sc-166297) were dropped on a tissue chip, which contained 90 pairs of HCC tissues and tumor-adjacent liver tissue. The chip was then placed in a moisture chamber at 4 ℃ overnight. Secondary antibodies (Thermo Fisher Scientific) at a 1:1,000 dilution were added to the tissue chip and incubated at room temperature for 30 min. Three representative images were achieved from each sample, and we invited a senior pathologist for further analysis.

Tumor xenografts

Females BALB/c nude mice (5 weeks old, weight: 18–21 g, Cyagen Biosciences lnc.) were used for the xenograft models. All of the mice were housed in SPF (Specific pathogen Free) conditions. For the *in vivo* siRNA treatment experiment, LEN-HeG2 cells (5×10^5 in 100 µL sterile PBS) were subcutaneously injected in the right flanks of each mouse. Next, the mice were randomized into two groups (n=4 in each group) when the tumor size reached approximately 100 mm^3, *in vivo* siRNA was delivered by intratumor injection twice a week at a dose of 5 nmol in each mouse. After 31 days, the mice were sacrificed and the tumors were obtained for further study. Animal experiments were performed under a project license (No. S20220228-004) granted by the Institute Ethics Committee at the Affiliated Hospital of Nantong University, in compliance with the guidance of the care and use of laboratory animals issued by the Ministry of Science and Technology of the China. A protocol was prepared before the study without registration.

Statistical analysis

R program (version 4.1.2) was used for all data visualization and statistical analysis. The mean and standard deviation (SD) from at least three different experiments were used to represent all of the data. One-way Analysis of Variance (ANOVA) or the student's *t*-test was utilized to assess the differences between several groups. Statistical significance was defined as $P<0.05$.

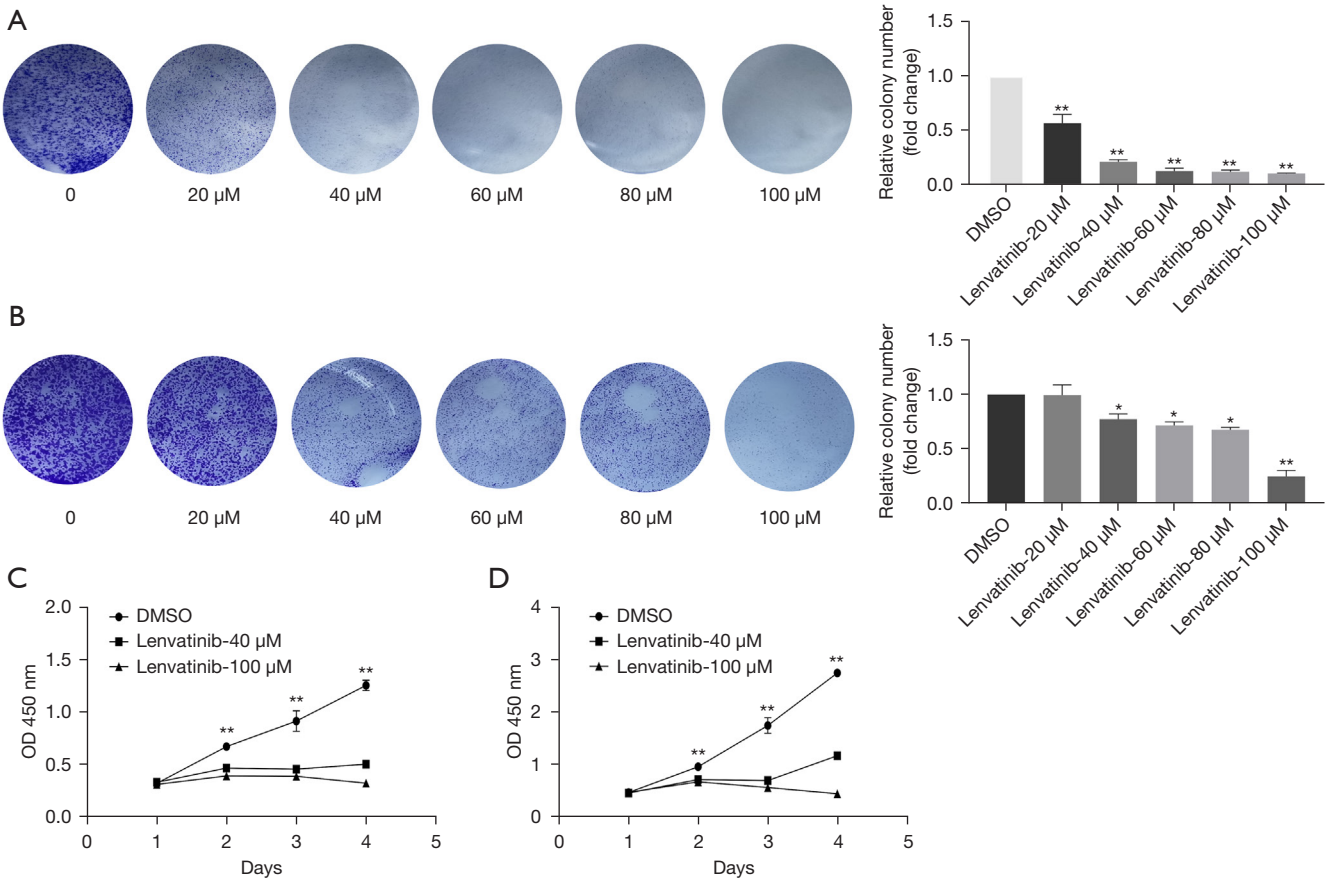

Figure 1 Inhibitory effect of lenvatinib on HCC cell proliferation. Different lenvatinib concentrations, i.e., 0, 20, 40, 60, 80, and 100 μM, and stain with crystal violet. Results display lenvatinib inhibited the proliferation of HCC cells. (A) Lenvatinib decreases the proliferation of LM3 cells at a low dose of 20 μM. (B) Lenvatinib decreases the proliferation of MHCC-97H cells at 40 μM. After methanol fixation, clones were stained with crystal violet. According to the CCK-8 assay, the proliferative rates of LM3 (C) and MHCC-97H (D) cells exposed to various concentrations of lenvatinib were evaluated. *P<0.05; **P<0.01. OD, optical density; HCC, hepatocellular carcinoma; DMSO, dimethyl sulfoxide.

Results

Lenvatinib inhibits the proliferation of HCC cells

To investigate the role of lenvatinib in HCC cells, a colony formation assay was used to determine the influence of lenvatinib on the proliferation of liver cancer cells. Different concentrations of lenvatinib were co-cultured with liver cancer cells for 2 weeks. At a low dose of 20 μM, lenvatinib dramatically decreased the proliferation of LM3 cells (*Figure 1A*) but only suppressed cell proliferation in MHCC-97H cells at doses higher than 40 μM (*Figure 1B*). Analysis of the growth curves of CCK-8 cells showed that lenvatinib suppressed the growth and proliferation of the LM3 and MHCC-97H HCC cell lines (*Figure 1C,1D*).

Identification and validation of targets for lenvatinib in HCC

To determine the drug target of lenvatinib, RNA-seq was employed to evaluate the transcriptome differences between lenvatinib-treated MHCC-97H cells and their parental counterparts. MHCC-97H cells treated with 40, 60, 80, and 100 μM lenvatinib were used for sequencing. The results showed that different significant genes affect the molecular function (MF, *Figure 2A*), cellular component (CC, *Figure 2B*), biological process (BP, *Figure 2C*), and KEGG (*Figure 2D*) pathways. Moreover, compared to their parental counterparts, LR MHCC-97H cells (LEN-MHCC-97H) had 42 up-regulated and 38 down-regulated DEGs (*Figure 3A*, Table S3). The PPI network of DEGs demonstrated that *AKR1C1* was the most prominent up-

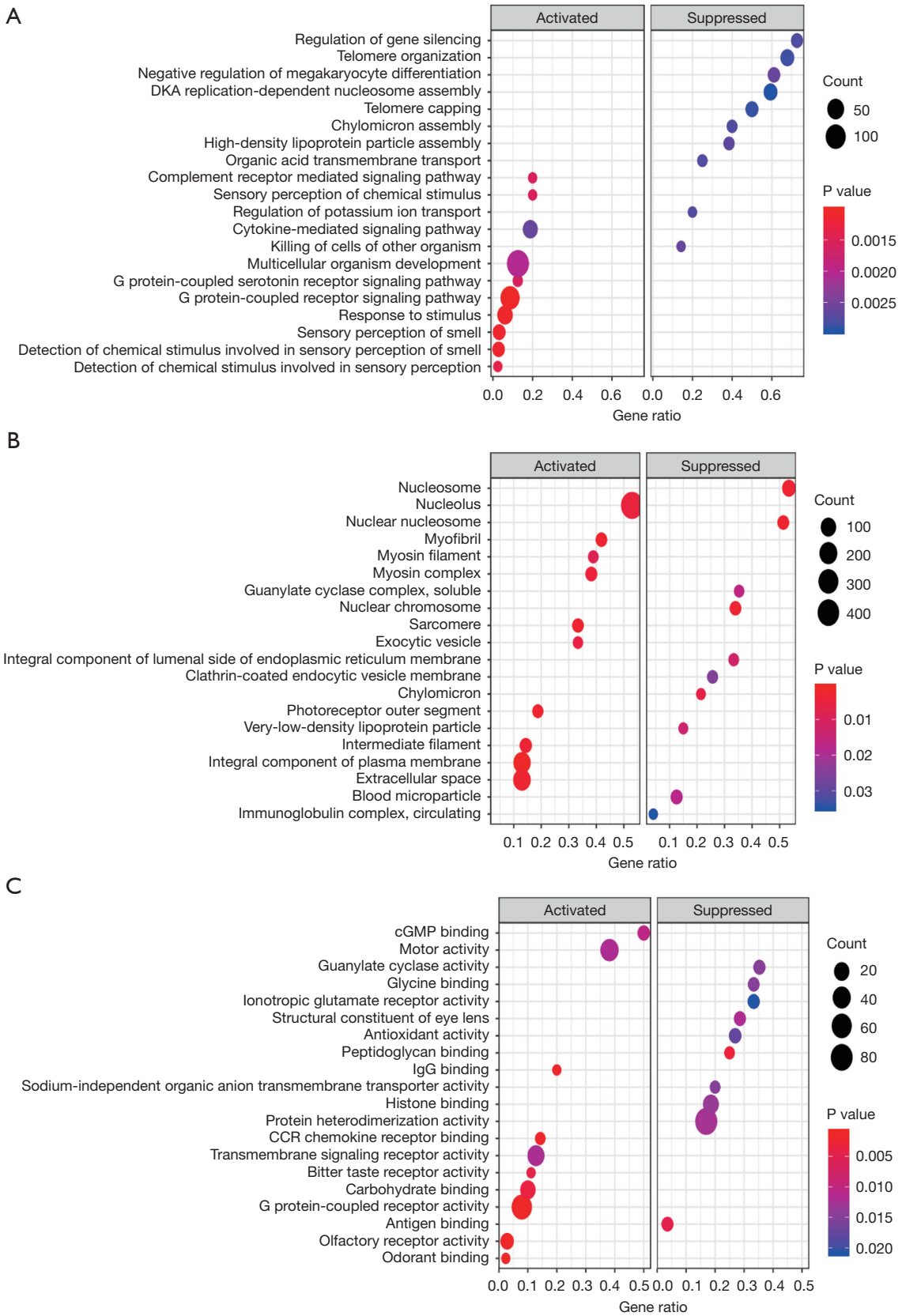

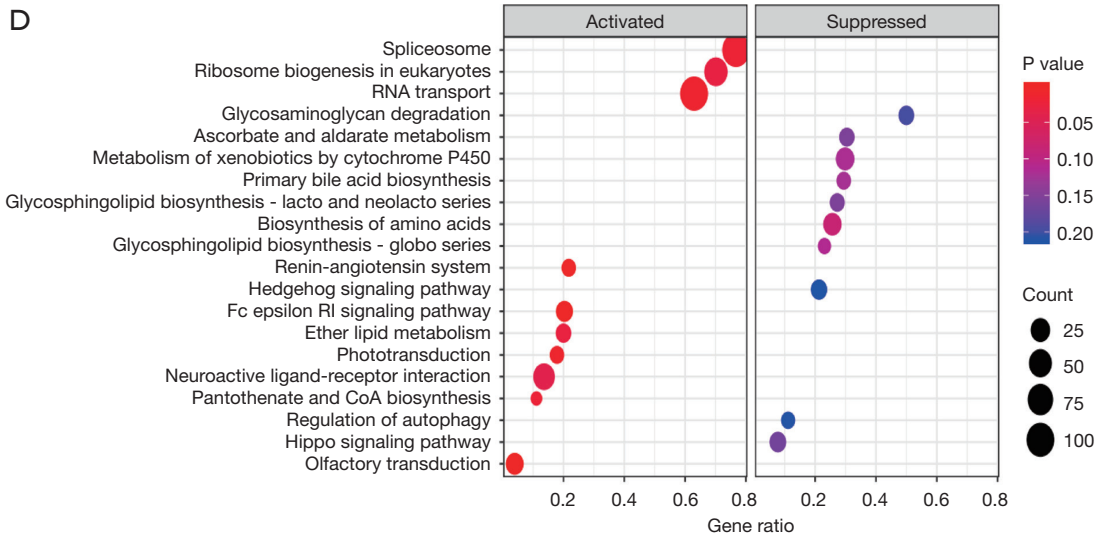

Figure 2 Identification and analysis of GO and KEGG terms of differentially expressed genes following RNA-seq. Bubble diagram of the top 10 activated or suppressed terms in biological process (A), cellular component (B), molecular function (C), and Kyoto Encyclopedia of Genes and Genomes enrichment (D). GO, Gene Ontology; KEGG, Kyoto Encyclopedia of Genes and Genomes.

regulated gene in LEN-MHCC-97H cells, and serpin family E member 1 (*SERPINE1*) was a considerably down-regulated gene in LEN-MHCC-97H cells (*Figure 3B,3C*, *Tables 2,3*). *SERPINE1* promotes the proliferation, invasion, migration, and epithelial-mesenchymal transition (EMT) of HCC cells (16,17). However, the function of *AKR1C1* in HCC is not clear.

The UALCAN (The University of ALabama at Birmingham CANcer data analysis Portal, http://ualcan.path.uab.edu) database was used to evaluate the link between *AKR1C1* and *SERPINE1*. Furthermore, their expressions with clinical features were also assessed (*Figure 3D,3E*). In HCC patients, high expression of *AKR1C1* and *SERPINE1* was linked to worse overall survival (OS). To learn more about the interconnected roles and processes of DEGs, KEGG pathway enrichment analysis was employed for the functional annotation of these genes. To further understand the biological significance of co-regulated proteins, KEGG pathway enrichment analyzed the collected expression data of *AKR1C1* and *SERPINE1* messenger RNA (mRNA) for HCC samples from TCGA dataset. The obtained results showed that *AKR1C1* is correlated with several tumor progression cascades, such as the *Wnt* signaling cascade, the calcium signaling system, the cascades that lead to gastric cancer, and so on (*Figure 3F*). In addition to its role in the *PI3K/AKT* signaling cascade, *SERPINE1* is also engaged in the *Wnt* signaling cascade, the *IL-17* signaling cascade, etc. (*Figure 3G*). The *Wnt* signaling pathway is shared by *AKR1C1* and *SERPINE1*, suggesting that lenvatinib may affect the progression of HCC through the *Wnt* signaling pathway.

The gene expression of downloaded samples was analyzed using CIBERSORT to estimate the levels of 22 different types of immune cells. This helped find differences in the expression levels between the low- and high-expression groups. For *AKR1C1*, the ratios of activated dendritic cells activated memory *CD4* T cells, and eosinophils were different between the two groups, and the proportions of macrophages (*M0*) were significantly higher in the high-expression group (*Figure 3H*). Moreover, for *SERPINE1* the ratios of the proportions of activated NK cells (natural killer cells), neutrophils, and activated mast cells were found to be changed in two groups. The proportions of macrophages (*M0*) and resting memory *CD4* T cells, were significantly elevated in the high-expression group, while the ratios of resting mast cells were considerably elevated in the low-expression group (*Figure 3I*). *AKR1C1* and *SERPINE1* were significantly correlated with at least one type of immune cell and were positively correlated with macrophages (*M0*) (*Figure 3J*). Taken together, the underlined data suggested that *AKR1C1* and *SERPINE1* may be crucial contributors to the development of HCC.

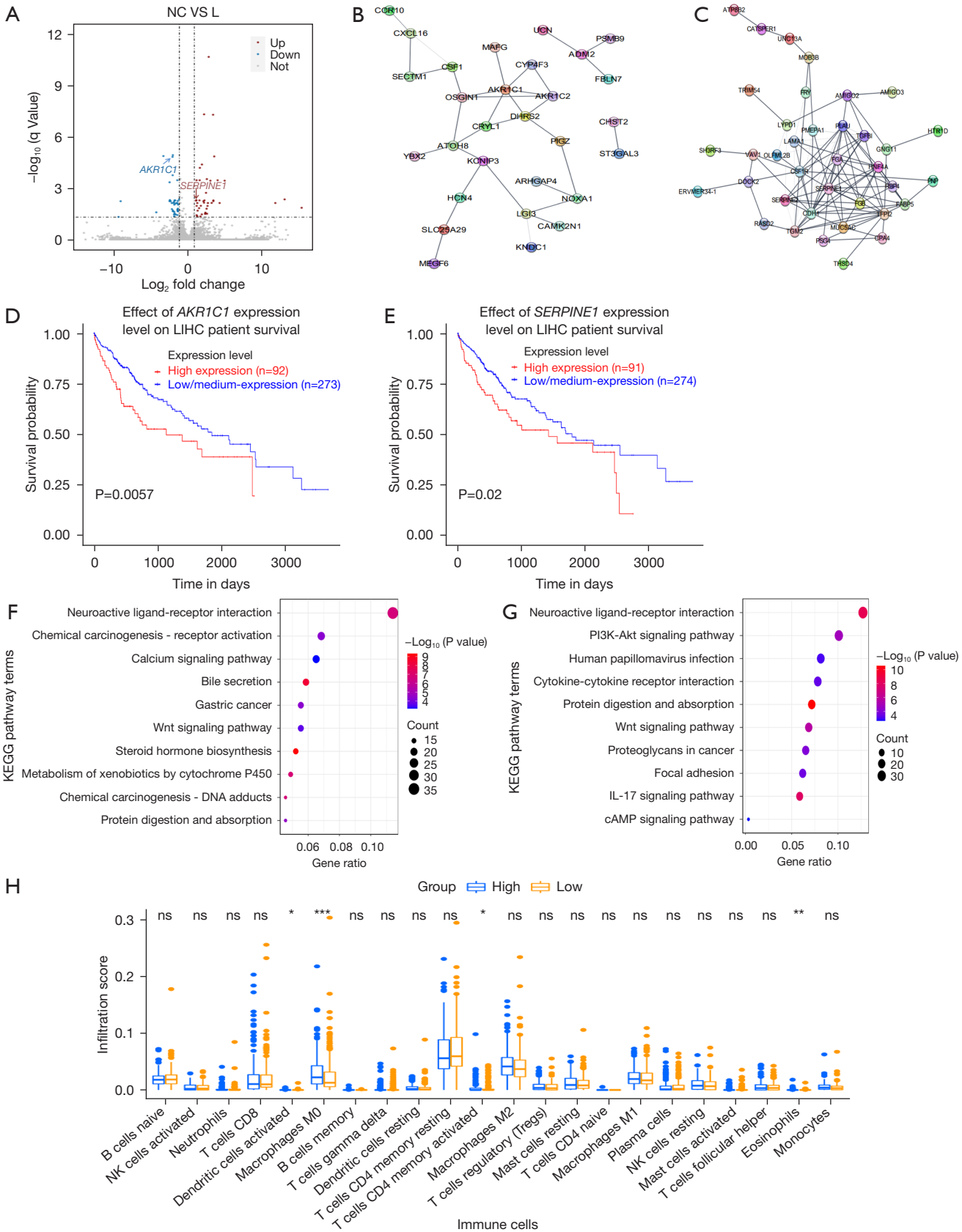

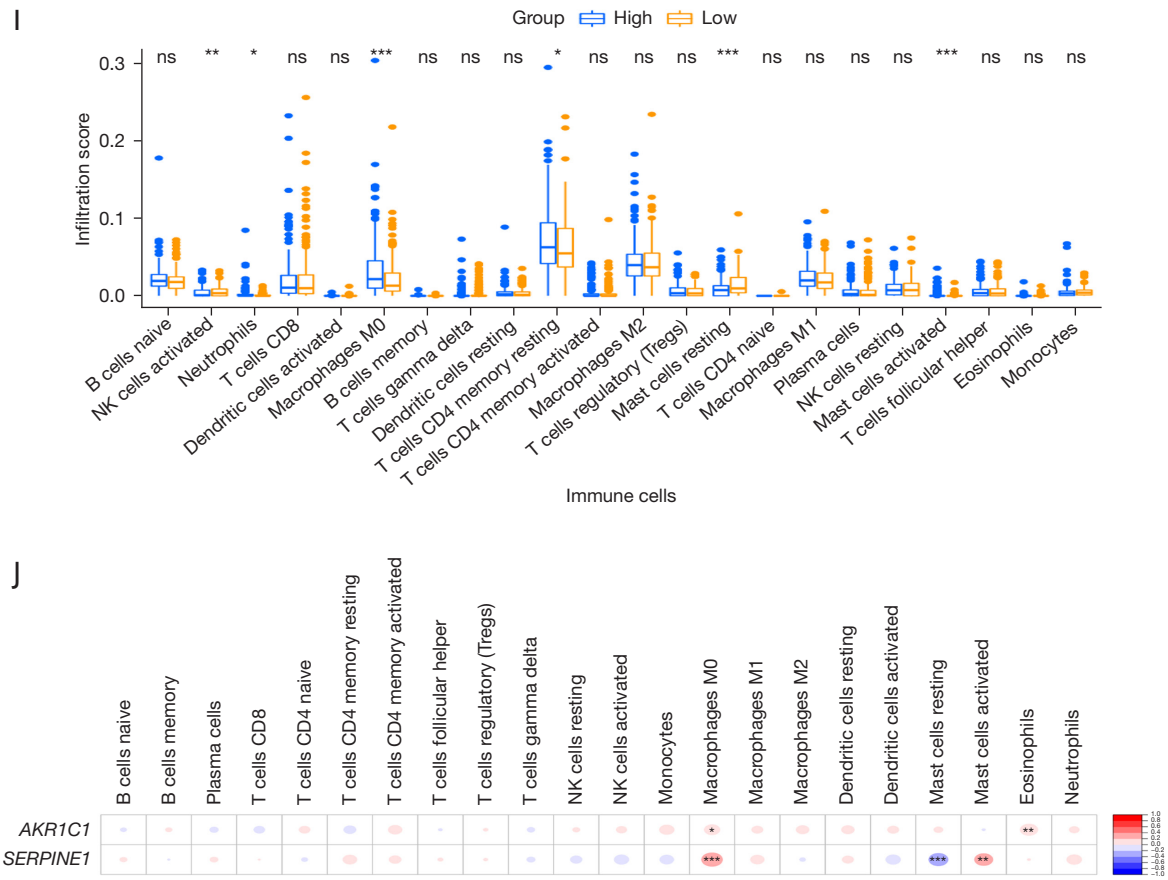

Figure 3 *AKR1C1* and *SERPINE1* were the key differentially expressed genes of lenvatinib targets. (A) RNA-seq was used to examine the transcriptome alterations in MHCC-97H cells treated with varying doses of lenvatinib. Genes with high or low expression in the four treatment groups were simultaneously shown by a volcano plot. Blue represents downregulated genes, red represents upregulated genes, and grey represents no difference genes. (B) The PPI network of the hub genes from upregulated genes. (C) PPI network of the hub genes from downregulated genes. (D,E) High expressions of *AKR1C1* and *SERPINE1* predicted poor prognosis in HCC patients. (F) The KEGG analysis revealed that *AKR1C1* is involved in the *Wnt* signaling pathway, calcium signaling pathway, gastric cancer, etc. (G) The KEGG analysis also showed that *AKR1C1* is involved in the *PI3K/AKT* signaling pathway, the Wnt signaling pathway, the *IL-17* signaling pathway, and other pathways. (H) According to the expression level of *AKR1C1*, the data were divided into two groups. The ratios of activated dendritic cells, macrophages (*M0*), activated memory *CD4* T cells, and eosinophils were characterized in two groups. (I) Similarly, for *SERPINE1*, the ratios of the proportions of activated NK cells, neutrophils, macrophages (*M0*), resting memory *CD4* T cell, resting mast cells, and activated mast cells showed marked changes. (J) *AKR1C1* and *SERPINE1* are significantly correlated with macrophages (*M0*) (red indicates that AKR1C1 and SERPINE1 expression are positively correlated with immune cells. Blue indicates that AKR1C1 and SERPINE1 expression are negatively correlated with immune cells. The larger the difference in the ratios of the proportions of immune cells, the larger the circle size). *P<0.05, **P<0.01, ***P<0.001. PPI, protein-protein interaction; KEGG, Kyoto Encyclopedia of Genes and Genomes; LIHC, liver cancer; HCC, hepatocellular carcinoma; NC, negative control; NS, no sense.

AKR1C1 was increased in LR HCC cells and HCC tissues

Hou *et al.* developed two LR (LR HCC cell lines, i.e., Hep3B_LR and Huh7_LR (18). Venn diagrams indicated that the *XDH*, *RAB20*, *ITGA3*, *GALNT6*, *NYNRIN*, *DCHS1*, and *FERMT1* genes were co-upregulated in both LR cell lines, and the *LINC00941*, *INHBB*, and *MYBPC3* genes were down-regulated collectively in both LR cell lines (*Figure 4A*,*4B*, *Table 4*).

Using *in vitro* experiments, drug-resistant cell lines can be established using either the low concentration gradient

Table 2 The top five up-regulated genes in LR-MHCC-97H cells

Gene symbol	Official full name	P value	log_2FoldChange	Degree
AKR1C1	Aldo-keto reductase family 1 member C1	7.63E-09	1.922757431	6
AKR1C2	Aldo-keto reductase family 1 member C2	4.52E-07	1.280578159	4
ATOH8	Atonal bHLH transcription factor 8	8.01E-05	2.00726935	4
DHRS2	Dehydrogenase/reductase 2	6.96E-07	2.319644624	4
LGI3	Leucine rich repeat LGI family member 3	1.04E-05	2.279837753	4

LR, lenvatinib-resistant.

Table 3 The top five down-regulated genes in LR-MHCC-97H cells

Gene symbol	Official full name	P value	Log_2FoldChange	Degree
SERPINE1	Serpin family E member 1	1.41E-05	–1.237791096	15
CDH1	Cadherin 1	4.75E-05	–2.777204459	14
TFPI2	Tissue factor pathway inhibitor 2	0.000152137	–2.493556172	13
TGM2	Transglutaminase 2	0.000191443	–2.45014128	13
TGFBI	Transforming growth factor beta induced	1.26E-05	–1.694486544	12

LR, lenvatinib-resistant.

rise or high dosage intermittent impact. In our previous study, we found that the expression of *AKR1C1* was increased in MHCC-97H cells co-cultured with different concentrations of lenvatinib, especially when co-cultured with lenvatinib at 100 μM. Simultaneously, the expression of *AKR1C1* was also enhanced in the drug-resistant hepatoma cells induced by low concentrations of lenvatinib from the GSE186191 dataset (*Figure 4C*,*4D*). To further verify these conclusions, HepG2_LR cell lines were established and the results demonstrated that the expression of *AKR1C1* was higher in HCC cells and also higher in LR cells than in the corresponding wild-type cells (*Figure 4E*). These findings suggest that *AKR1C1* can be used as a marker of lenvatinib resistance in HCC.

Immunohistochemistry was applied to detect the expression of *AKR1C1* in HCC tissue chips. We observed that the expression of *AKR1C1* was different between the HCC tissue and the tumor-adjacent liver tissue (*Figure 5A*). AKR1C1 has an immunostaining score of 0 to 12, using the product of the percentage of tumor cells with positive staining and staining intensity as the criterion. The expression level of AKR1C1 was determined by staining intensity (no staining, 0; Light staining, 1 point; Medium staining, 2 points; Heavy staining, 3 points) (*Figure 5B*), percentage of stained cells in cell count (<5%, 0 points; 5–25%, 1; 26–50%, 2 points; 51–75%, 3 points; >75%, 4 points). Multiply the two points to get a positive level. A total score greater than 6 indicates high AKR1C1 expression, while a score less than or equal to 6 indicates low AKR1C1 expression. In the 90 pairs of tissue sections in this study, there was a statistically significant difference in AKR1C1 expression between HCC tissues and liver tissues adjacent to tumors (*Figure 5C*). In addition, patients were divided into high AKR1C1 expression group and low AKR1C1 expression group based on the expression of AKR1C1 in HCC tissues relative to tumor adjacent liver tissues of HCC patients. Combined with the clinicopathological data of the patients, the results showed that *AKR1C1* expression was closely related to cirrhosis, tumor number, lymph gland metastasis, and the Tumor Node Metastasis (TNM) stage of HCC patients (P<0.05, *Table 5*). The overall survival rates of patients in the high *AKR1C1* expression group were significantly lower than those in the low *AKR1C1* expression group (*Figure 5D*).

Low expression of AKR1C1 inhibits the proliferation of HCC cells

The roles of *AKR1C1* in the proliferation of LEN-HepG2 cells were respectively analyzed by a CCK-8, wound healing

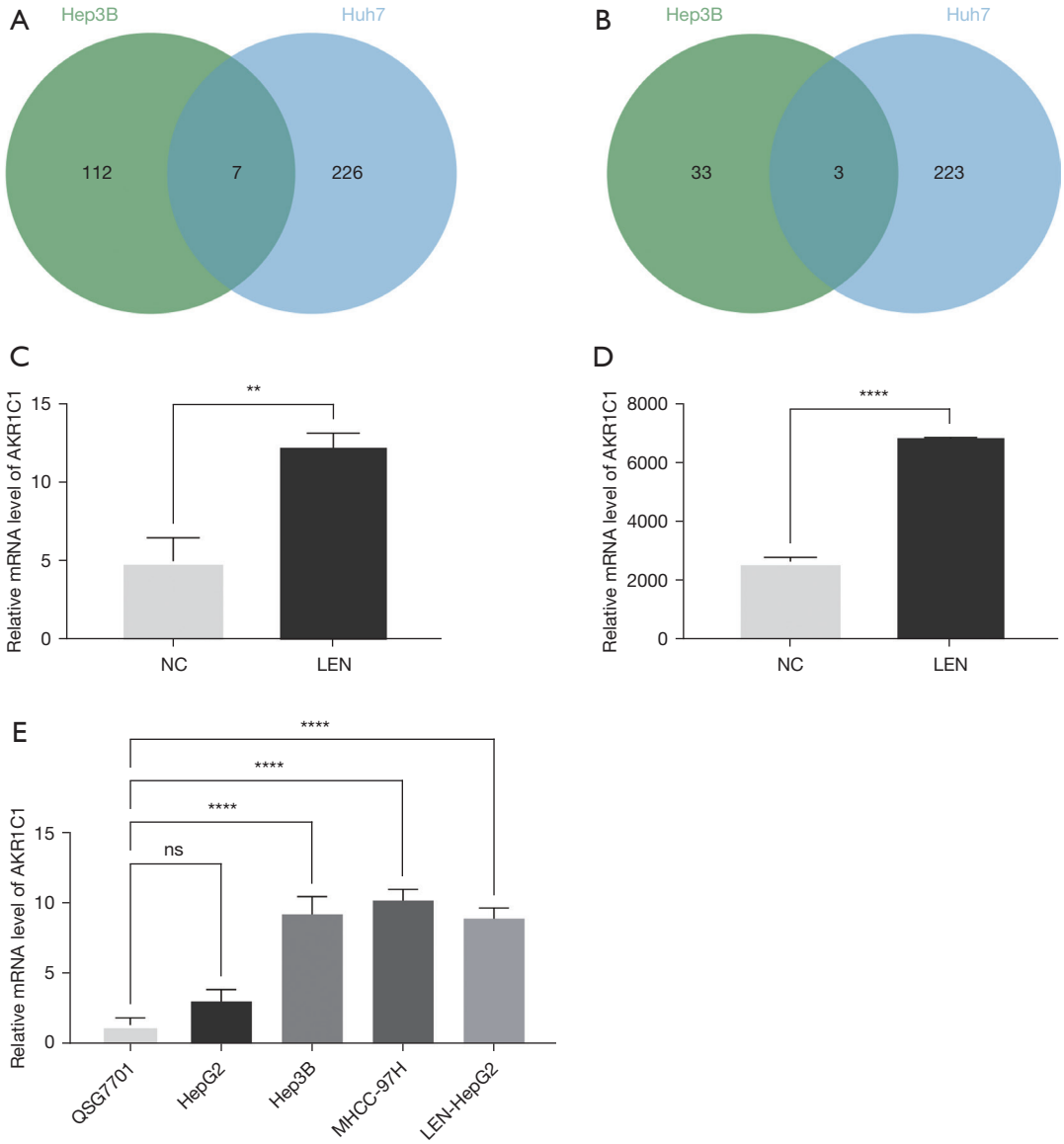

Figure 4 The *AKR1C1* expression was elevated in LR-HCC cells. (A) Seven up-regulated genes in LR Hep3B and Huh7 cells. (B) Three down-regulated genes in LR Hep3B and Huh7 cells. *AKR1C1* was increased in HCC cell lines that were resistant to lenvatinib compared with the control group, (C) Hep3B, and (D) Huh7, respectively. (E) *AKR1C1* was elevated in HCC cells and LEN-HepG2 (LR-HepG2 cells). **P<0.01, ****P<0.0001. LR, lenvatinib-resistant; HCC, hepatocellular carcinoma; NC, negative control; LEN, lenvatinib; NS, no sense.

assay, and EdU. First, we found that in comparison to the siNC group (control group), *AKR1C1* mRNA expression in LEN-HepG2 was downregulated after transduction with *AKR1C1* siRNA (*Figure 6A*). The CCK-8 assays showed that LEN-HepG2 cell viability was notably lower in the knockdown group compared with the siNC group (*Figure 6B*). Furthermore, the wound healing and EdU assays (*Figure 6C*,*6D*) displayed the same results. Meanwhile, in MHCC-97H cells, the knockdown of *AKR1C1* also decreased the proliferation and migration ability of MHCC-97H cells (*Figure 7A*). CCK-8 assays revealed that cell proliferation of MHCC-97H cells was notably reduced after transduction (*Figure 7B*). In addition, the wound healing (*Figure 7C*) and EdU (*Figure 7D*) assays also showed the same results.

We then calculated the weights and volumes of the

Table 4 Abnormally expressed genes in LR Hep3B and Huh7 cells

Highly expressed genes in LR HCC cells
Xanthine dehydrogenase (*XDH*)
Member RAS oncogene family (*RAB20*)
Integrin subunit alpha 3 (*ITGA3*)
Polypeptide N-acetylgalactosaminyltransferase 6 (*GALNT6*)
NYN domain and retroviral integrase containing (*NYNRIN*)
Dachsous cadherin-related 1 (*DCHS1*)
FERM domain containing kindlin 1 (*FERMT1*)
Lowly expressed genes in LR HCC cells
Long intergenic non-protein coding RNA 941 (*LINC00941*)
Inhibin subunit beta B (*INHBB*)
Myosin binding protein C3 (*MYBPC3*)

LR, lenvatinib-resistant; HCC, hepatocellular carcinoma.

tumors to explore the roles of *AKR1C1* in the tumor growth of HCC cells *in vivo*. Our results showed that the *AKR1C1* siRNA group had a reduced tumor weight and volume compared with the siNC group (*Figure 8A-8C*). Also, immunohistochemistry staining revealed elevated expressions of proliferating cell nuclear antigen (*PCNA*) and *N-cadherin* and a reduced expression level of *E-cadherin* in the siNC group (*Figure 8D*).

MiRNA prediction

MiRNAs are epigenetic regulators that have shown enormous potential as therapeutic targets for a variety of human diseases and are the subject of extensive research (19). They play essential roles in processes related to tumor growth, including proliferation, angiogenesis, and invasion (20). The microRNA data integration portal (mirDIP) and starBase databases were utilized to predict the interactions between miRNAs and *AKR1C1* (Table S4), and only one miRNA, i.e., *miR-4644*, was identified (*Figure 9A*). It was also found that *miR-4644* expression was elevated in LR cells compared with the corresponding wild-type cells (*Figure 9B*). According to reports from Zhao *et al.*, *miR-4644* has higher stability and expression abundance than other regularly used reference controls, making it an effective endogenous normalizer for circulating microRNA quantification in HCC (21). Considering the elevated level of *miR-4644* expression in LR cells, circulating *miR-4644* may be a promising biomarker for the early diagnosis of LR.

Extensive evidence from numerous sources confirms that long non-coding RNAs (lncRNAs) are crucial in the development of HCC treatment resistance (22,23). It was previously reported that the expression of *LINC00941* was reduced in LR cells (*Table 4*); therefore, we used the database to further investigate the lncRNAs that interacted with regulator miRNAs and generated lncRNA-miRNA subnetworks (*Figure 9C*). Interestingly, it was determined that several lncRNAs enhance cell proliferation in the development of hepatic carcinogenesis, such as taurine up-regulated 1 (*TUG1*) (24), and human leukocyte antigen (HLA) complex group 18 (*HCG18*) (25).

Erastin inhibits the expression of AKR1C1 in HepG2 cells

Studies have revealed that *AKR1C1* is linked to numerous ferroptosis-associated cancers, such as glioblastoma (26), colon adenocarcinoma (27), non-small cell lung cancer (28), breast cancer (29) and clear cell renal cell carcinoma (30). Recent research has indicated that sorafenib can elicit ferroptosis, a type of programmed cell death characterized by iron-dependent lipid peroxide accumulation (31,32). Our results showed that erastin treatment inhibits the *AKR1C1* expression in HepG2 cells from the GSE104462 dataset (*Figure 10A*) (33). Our experiment demonstrated that different concentrations of erastin can inhibit the expression of *AKR1C1* in LEN-HepG2 cells (*Figure 10B*). In addition, sorafenib, which was the earliest approved first-line treatment for advanced HCC (34), also inhibits the expression of *AKR1C1* in LEN-HepG2 cells (*Figure 10C*). This suggests that LR patients who exhibit elevated *AKR1C1* expression can be treated with sorafenib, but more experiments to verify this viewpoint.

Prediction of drug sensitivity associated with AKR1C1

Considering the probable role of *AKR1C1* in regulating medication sensitivity, we investigated whether individuals in different risk categories had varying levels of sensitivity to various cancer drugs. Each HCC patient's IC_{50} value was predicted using the prediction model. Taking IC_{50} <1 as the screening criterion, we were able to narrow down the number of prospective anticancer medicines to 11. This means that these compounds have a strong inhibitory effect on HCC (*Figure 11A*). The response to five of these medications varied in the various risk categories with a statistically significant P value <0.05 (*Figure 11B*). Other than SN-38 (7-ethyl-10-hydroxycamptothecin), the

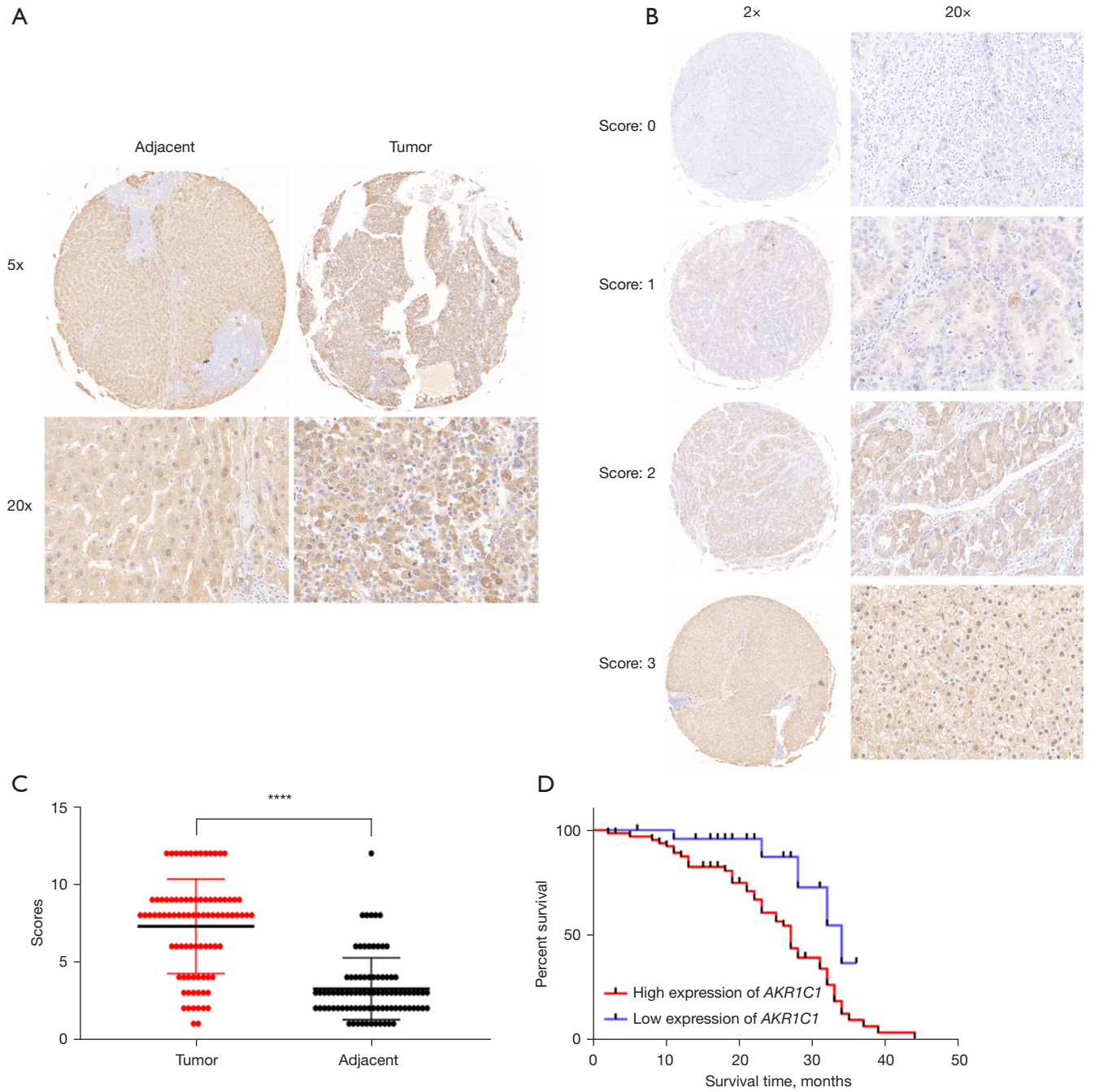

Figure 5 Analysis of *AKR1C1* expression in human HCC tissues and the survival of HCC patients. (A) Expression of *AKR1C1* in human HCC tissues and paracancerous tissues (IHC staining). (B) Staining scores of *AKR1C1* expression in HCC tissue samples and surrounding noncancerous tissues (IHC staining). (C) The immunostaining scores of *AKR1C1* in 90 pairs of human HCC tissues and paracancerous tissues (****P<0.0001). (D) Kaplan-Meier analysis of the overall survival outcomes for 90 pairs of human HCC tissues (P=0.0198). *P<0.05, **P<0.01. HCC, hepatocellular carcinoma; TNM, International Classification of Clinical Stages for Malignant Tumors; AFP, alpha-fetoprotein.

Table 5 Relationship between the expression of AKR1C1 in HCC tissues and the clinical characteristics of HCC patients

Parameters	High-expression group (n=56)	Low-expression group (n=34)	P
Age (years)			0.3615
≤60 (n=29)	16	13	
>60 (n=61)	40	21	
Gender			0.8068
Male (n=67)	41	26	
Female (n=23)	15	8	
AFP (μg/L)			>0.9999
≤20 (n=31)	19	12	
>20 (n=59)	37	22	
Cirrhosis			0.0011**
Negative (n=22)	7	15	
Positive (n=68)	49	19	
Tumor number			0.0101*
≤1 (n=62)	33	29	
>1 (n=28)	23	5	
Lymph gland metastasis			0.0032**
Negative (n=56)	28	28	
Positive (n=34)	28	6	
TNM stage			0.0204*
I/II (n=60)	32	28	
III (n=30)	24	6	

*P<0.05, **P<0.01. HCC, hepatocellular carcinoma; TNM, tumour-node-metastasis; AFP, alpha-fetoprotein.

majority of the medications, such as trametinib, vinorelbine, sepantronium bromide, and luminespib, displayed greater IC_{50} values in the high-risk groups than in the low-risk groups, indicating that SN-38 patients were more likely to respond appropriately.

Discussion

Patients with cirrhosis have an increased risk of developing HCC, and those with a single tumor and healthy liver function make the best resection candidates. The conventional treatments for advanced HCC are sorafenib, lenvatinib, and regorafenib, as they increase the patient's survival rate (35). Lenvatinib, an oral small molecule inhibitor of several receptor tyrosine kinases, has been approved in the United States, the European Union, Japan, and China as the first-line therapy in patients with unresectable HCC. Lenvatinib significantly improves the objective response rate (ORR), progression-free survival (PFS), and time to progression (TTP) compared to sorafenib therapy (36). At present, HCC treatment is challenging because of the lack of understanding of the molecular mechanisms of lenvatinib resistance in HCC, which occurs often in both primary and acquired forms.

In this study, we first confirmed that lenvatinib inhibits the proliferation of HCC cells. To explore the underlying molecular mechanism that mediates the phenotypic changes, RNA-seq was used to compare the transcriptomes of MHCC-97H cells exposed to varying doses of lenvatinib with those of their parental counterparts. We identified two of the most valuable genes, i.e., *AKR1C1* and *SERPINE1*. When HCC cells were exposed to various doses of lenvatinib, the expression of *AKR1C1* was upregulated, while that of *SERPINE1* was downregulated. According to the obtained results, lenvatinib can inhibit the expression of *SERPINE1* (an oncogene in HCC) in HCC cells, regardless of the concentration (16,17) This indicated that *SERPINE1* was the target of lenvatinib, and in HCC patients with a high expression of *SERPINE1*, lenvatinib can be used for targeted treatment. In contrast, *AKR1C1* was increased in HCC cells treated with varying doses of lenvatinib, and the prognosis of HCC patients with high expression of *AKR1C1* was poor. Therefore, it is suggested that *AKR1C1* may induce lenvatinib resistance in HCC cells.

The KEGG links genomic data with higher-order functional data to analyze genes in a systematic way (37). Studies have confirmed that lenvatinib can regulate programmed cell death 1 ligand 1 (*PD-L1*) levels and regulatory T cells (Treg) differentiation in HCC (38), and CIBERSORT can accurately estimate the immune composition of a tumor biopsy (39). In this study, KEGG pathway enrichment analysis was performed to retrieve the expression data of *AKR1C1* and *SERPINE1* mRNA in HCC samples from TCGA database to better understand the biological function of HCC. Moreover, we also assessed the immune response of 22 TIICs using CIBERSORT. The *Wnt/β-catenin* pathway is typically upregulated in HCC and has been linked to tumor-initiating cell maintenance, tumor progression, drug resistance, and metastasis (40). KEGG analysis revealed that the Wnt signaling pathway is shared by *AKR1C1* and *SERPINE1*, which indicates that this pathway plays an important role in the treatment of

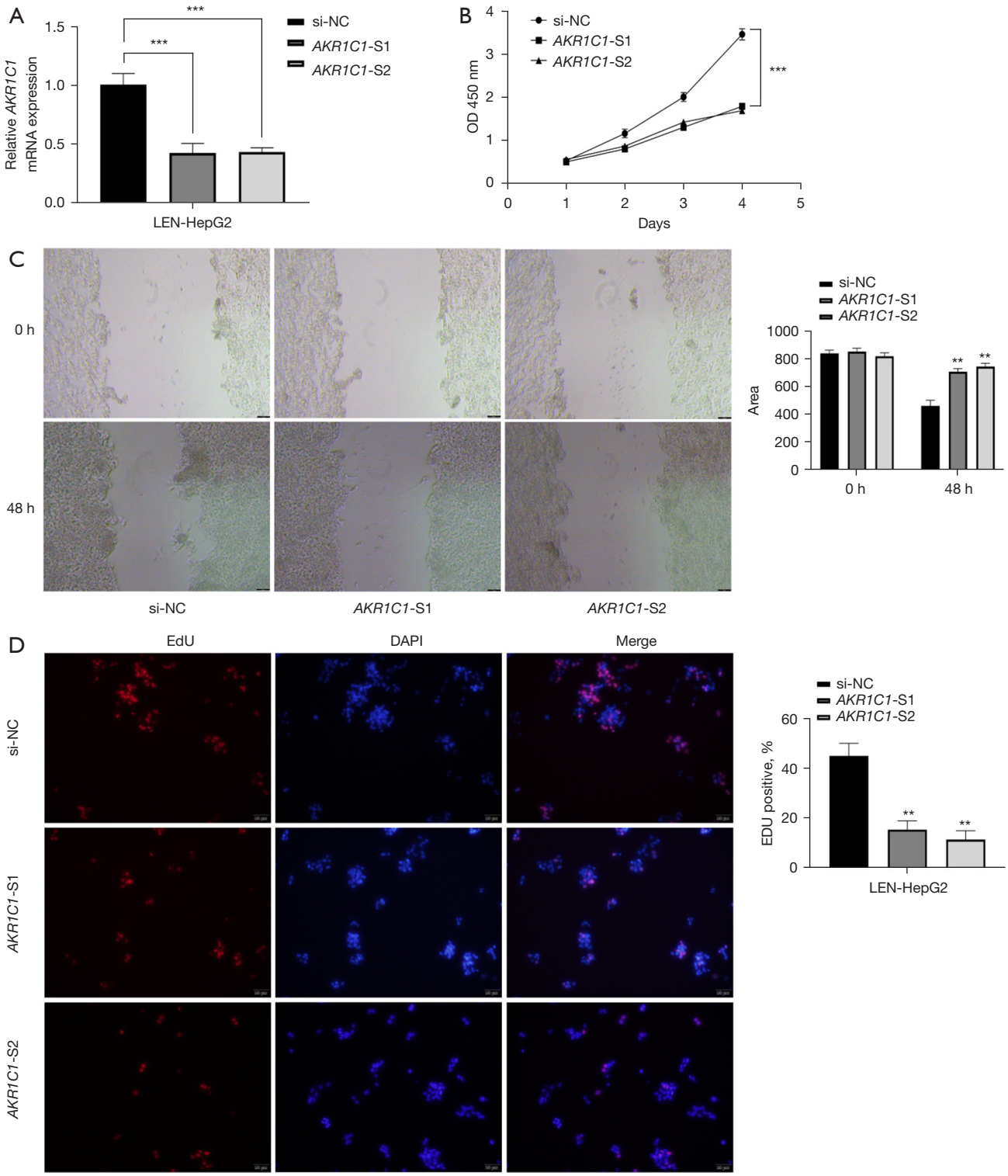

Figure 6 Knockdown of *AKR1C1* inhibits the proliferation of LEN-HepG2 cells. (A) The mRNA expression level of *AKR1C1* in LEN-HepG2 cells was determined by qRT-PCR analysis after transduction. The proliferation of LEN-HepG2 cells was assessed by CCK-8 assays (B), wound healing assay (C; ×100), and EdU (D; ×100), respectively. **P<0.01, ***P<0.001. NC, negative control; OD, optical density; EdU, 5-ethynyl-2'-deoxyuridine.

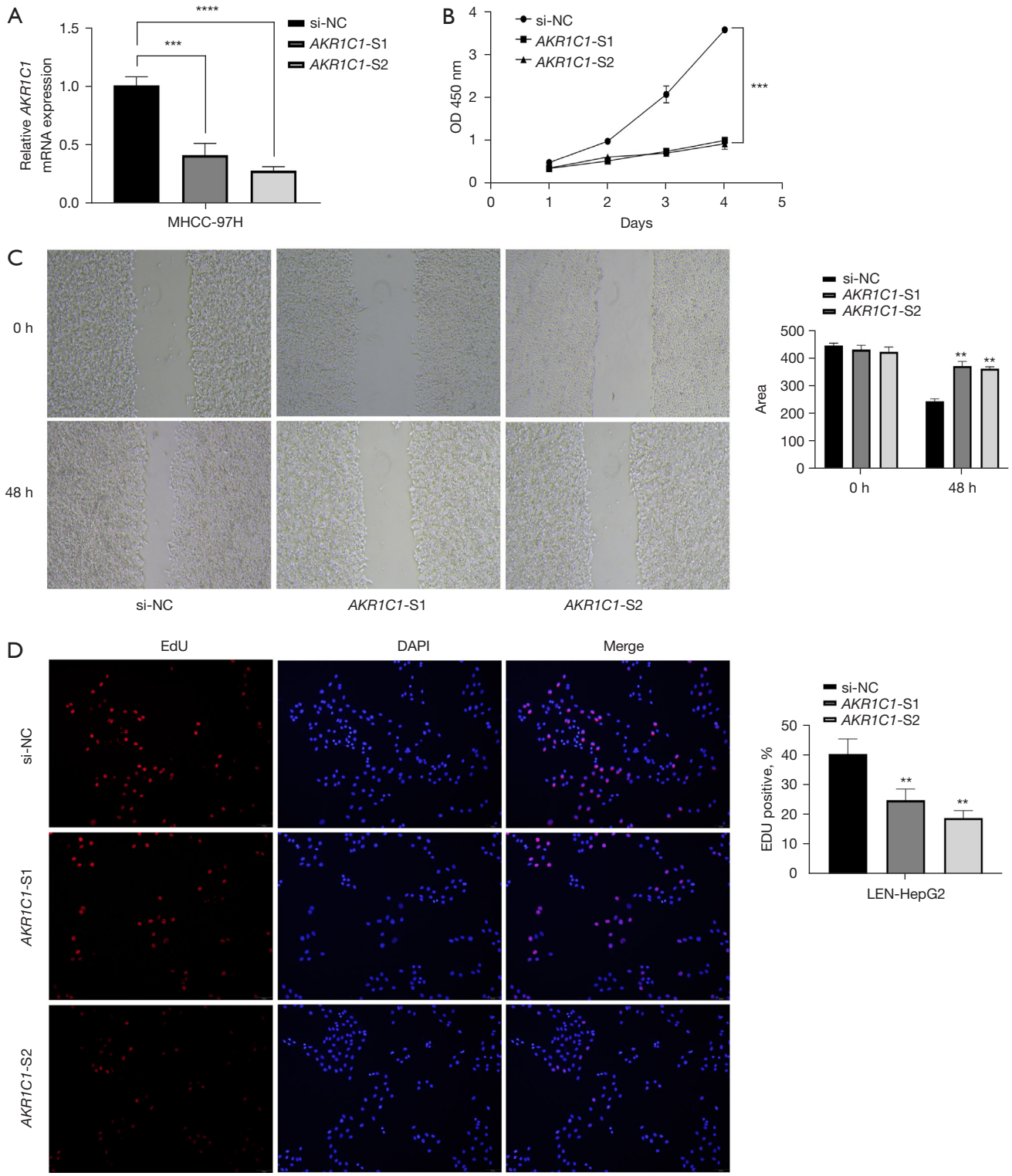

Figure 7 Knockdown of *AKR1C1* inhibits the proliferation of MHCC-97H cells. (A) The mRNA expression level of *AKR1C1* in MHCC-97H cells was determined by qRT-PCR analysis after transduction. The proliferation of MHCC-97H cells was assessed by CCK-8 assays (B), wound healing assay (C), and EdU (D), respectively (×20). **P<0.01, ***P<0.001, ****P<0.0001. NC, negative control; OD, optical density; EdU, 5-ethynyl-2'-deoxyuridine; DAPI, 4'-6-diamidino-2-phenylindole.

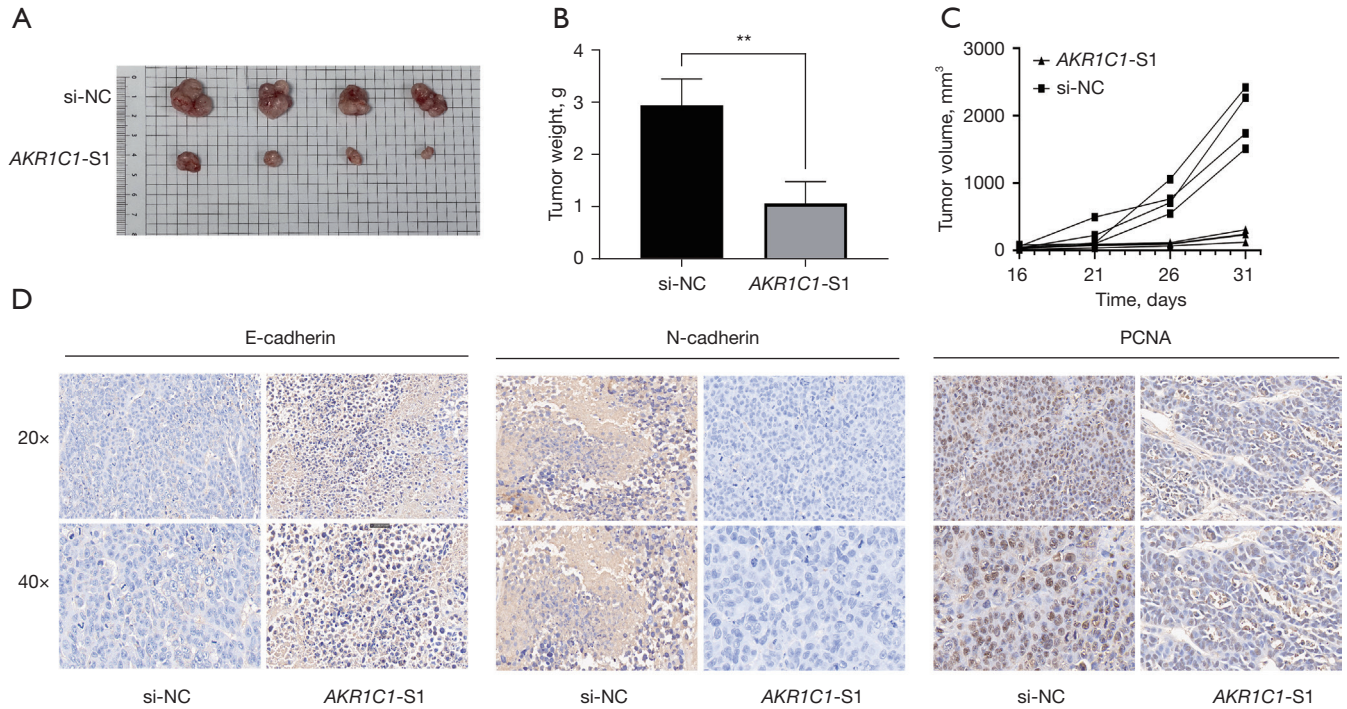

Figure 8 Knockdown of *AKR1C1* inhibits the proliferation of HCC cells *in vivo*. (A) Images of tumors in the *AKR1C1* knockdown and the control groups. (B,C) Knockdown of *AKR1C1* causes a significant decrease in tumor weight and volume (**P<0.01). (D) IHC staining images of *E-cadherin*, *N-cadherin*, and *PCNA* in the xenograft tumor tissues from each group of mice. HCC, hepatocellular carcinoma; NC, negative control; IHC, immunohistochemistry; PCNA, proliferating cell nuclear antigen.

HCC using lenvatinib. Compared to healthy liver tissues, the infiltration of *M0* macrophages was noticeably higher in HCC tissues. Correlation analysis showed that *M0* macrophage-related genes (M0RGs) had positive associations with immune cell infiltration, immune checkpoint inhibitory targets, clinicopathological characteristics, and the efficacy of common drugs (41). Resting-state macrophages (*M0*), which originate in the bone marrow, are typically regarded as precursors of polarized macrophages. M0-like macrophages are considered a feature of tumor malignancy (42). Additionally, these macrophages may act as a biomarker for HCC carcinogenesis, progression, and clinical results (43). CIBERSORT showed *AKR1C1* and *SERPINE1* are significantly correlated with *M0* macrophages, which revealed that these two genes act as potential characteristic markers of HCC that are enriched in *M0* macrophages.

The drug resistance of lenvatinib in HCC has recently gained increasing attention (18,44). By investigating the underlying molecular basis of lenvatinib resistance, we detected genes with abnormal expression in the GEO186191 dataset and the RNA-seq data for parental and LR HCC cells. We found that *XDH*, *RAB20*, *ITGA3*, *GALNT6*, *NYNRIN*, *DCHS1*, and *FERMT1* were co-upregulated genes, and *LINC00941*, *INHBB*, and *MYBPC3* were co-downregulated genes in both LR cell lines. This finding demonstrated that the *XDH*, *RAB20*, *ITGA3*, *GALNT6*, *NYNRIN*, *DCHS1*, and *FERMT1* genes may be targets of lenvatinib resistance, as genes with up-expression in drug-resistant cell lines possess a possible mechanism of producing drug resistance. However, we discovered that *XDH* (45), *RAB20* (46), and *ITGA3* (47) were downregulated and inhibited HCC cell proliferation; previous evidence suggests that these genes exert a tumor-suppressive function. Similarly, *LINC00941*'s activity as an oncogene is decreased in drug-resistant cell lines (48). Guan *et al.* considered that under the stimulation of sorafenib, the tumor suppressor gene *TSC2* becomes a "tumor-promoting factor" and then mediates the transmission of drug resistance signals (49), which implies that, like sorafenib resistance, the tumor microenvironment of LR patients has changed and requires personalized targeted therapy.

In the GEO186191 dataset, we found that the expression

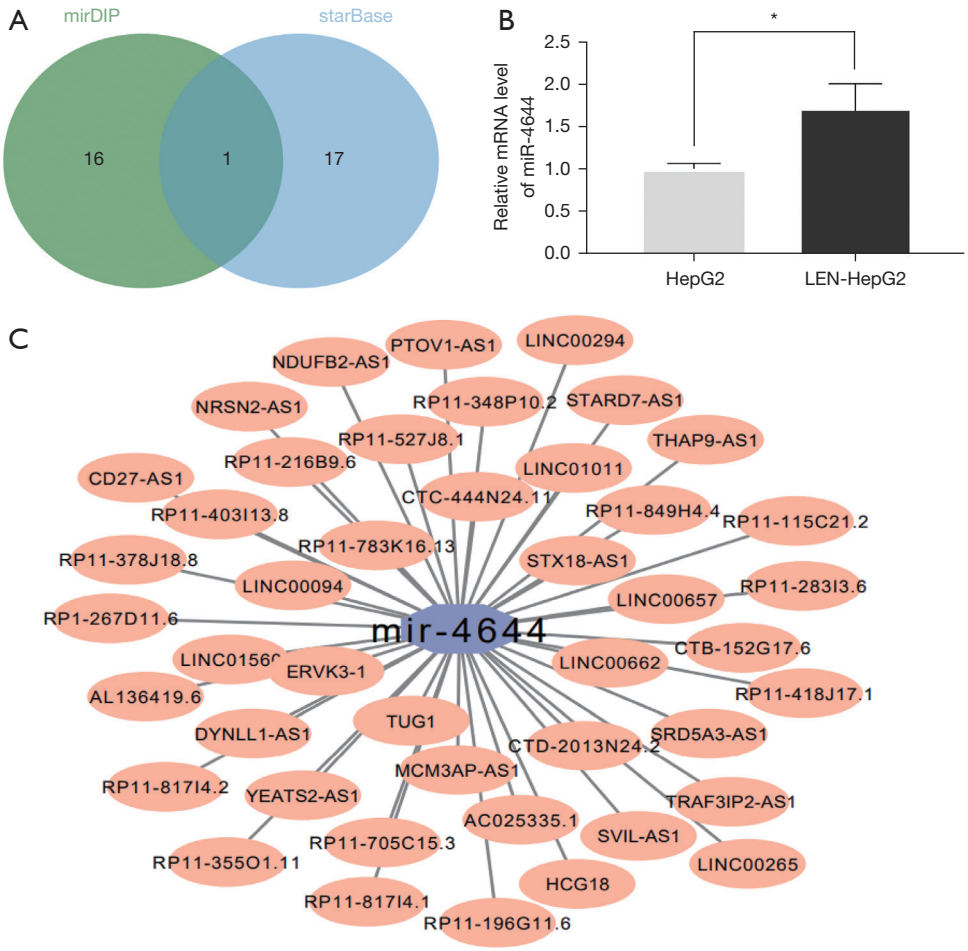

Figure 9 *MiR-4644* may be a biomarker for the early diagnosis of LR in HCC. (A) The mirDIP and starBase databases predicted that *miR-4644* may bind to *AKR1C1*; (B) in cells that have developed resistance to lenvatinib, *miR-4644* expression was significantly higher than in their wild-type counterparts; (C) prediction of the lncRNA-miRNA network in HCC. *P<0.05. LR, lenvatinib-resistant; HCC, hepatocellular carcinoma.

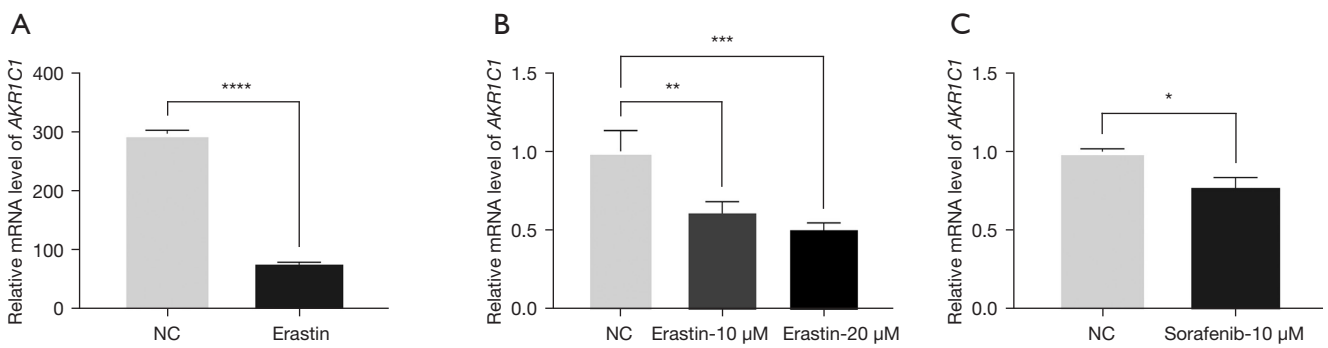

Figure 10 Erastin or sorafenib suppressed *AKR1C1* expression in HCC cells. (A) GSE104462 shows that erastin suppressed *AKR1C1* expression in HepG2 cells. (B) Different concentrations of erastin were co-cultured with LEN-HepG2 cells for 24 h. According to the results, erastin suppressed *AKR1C1* expression in LEN-HepG2 cells. (C) Sorafenib suppressed *AKR1C1* expression in LEN-HepG2 cells after being co-cultured for 24 h. *P<0.05, **P<0.01, ***P<0.001, ****P<0.0001. NC, negative control.

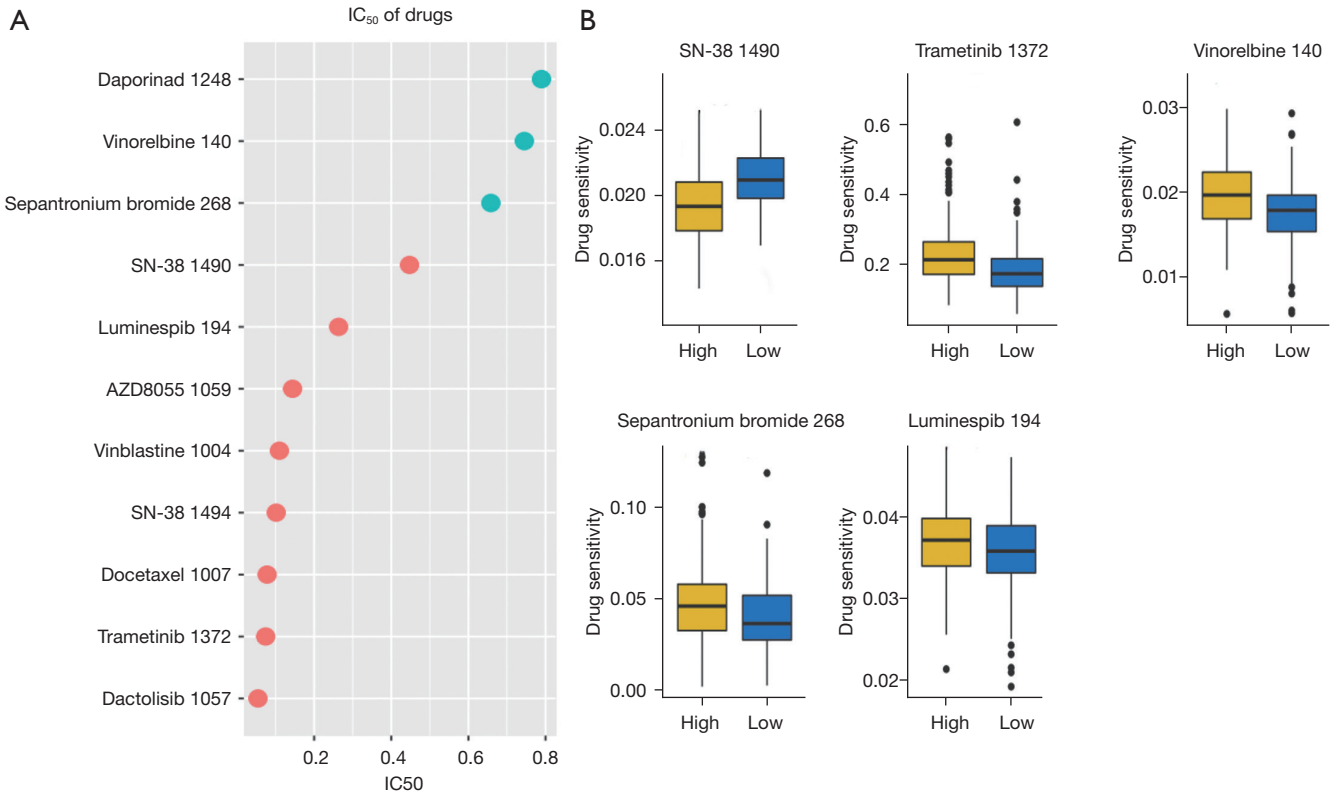

Figure 11 A drug sensitivity analysis. (A) Drug sensitivity analyses (IC_{50}<1). (B) Potential drugs with remarkable treatment variations between the high- and low-risk populations. The P value of each group is less than 0.05.

of *AKR1C1* was elevated in the drug-resistant HCC cells. Moreover, our results also showed that *AKR1C1* was highly expressed in HCC cells and LR cells. In our study, *AKR1C1* was overexpressed in HCC tissues, and high expression of *AKR1C1* predicts a poor outcome. Furthermore, *in vitro* experiments confirmed that the knockdown of *AKR1C1* inhibits the proliferation of LEN-HepG2 and MHCC-97H cells. According to these results, *AKR1C1* plays a pivotal role in LR in HCC cells. Moreover, *miR-4644* was identified and is highly expressed in LR cells compared with the corresponding wild-type cells. This is contrary to the competitive endogenous RNAs (ceRNA) network. Therefore, this study proposes two hypotheses. Firstly, miRNA may also function to induce gene expression (50), and *miR-4644* may target the *AKR1C1* promoter site and induce *AKR1C1* expression. Secondly, transcription factors involved in the regulation of *AKR1C1* are regulated by *miR-4644*; *miR-4644* and *AKR1C1* do not bind directly. According to the results of this study, *miR-4644* may act as a circulating microRNA to predict LR in HCC. However, there is still a need for further study to confirm this.

Additionally, this study revealed that *AKR1C1* was associated with multiple pathways that were linked to ferroptosis in different types of cancers (28,29). Ferroptosis is an iron-dependent regulatory cell death that is induced by severe lipid peroxidation (51). Erastin (an inducer of ferroptosis) inhibits the expression of *AKR1C1* in HepG2 cells. Considering that sorafenib can induce ferroptosis in HCC (52), we speculate that sorafenib can treat HCC patients with an elevated level of *AKR1C1* expression and individuals who are resistant to lenvatinib. Meanwhile, the GDSC database indicated that SN-38 was more likely to respond well in the high *AKR1C1* expression group. SN-38 is a semi-synthetic hydroxycamptothecin anti-tumor active substance, which can specifically bind to topoisomerase I to inhibit the synthesis of DNA in tumor cells. Irinotecan (CPT-11) as a clinical application preparation was first developed in Japan; it can release the prototype drug SN-38 with anti-cancer activity in the human body under the catalysis of carboxylesterase (53). Moreover, a study has shown that SN-38 and sorafenib have synergistic anticancer activity on HCC cells *in vitro* by augmenting apoptosis (54).

According to our previous study, sorafenib can inhibit the expression of *AKR1C1*. The results obtained in this study demonstrated that a combination of SN-38 and sorafenib is a possible approach to treat LR in HCC. Other study found that neurofibromin 1 (NF1), and dual specificity phosphatase 9 (DUSP9), as critical drivers for lenvatinib resistance in HCC (55). However, these are trial treatments following LR; the role of LR sensitivity in HCC needs to be validated by extensive studies. Next, we will use more experiments to verify our viewpoint.

Conclusions

Taken together, this study found that *AKR1C1* has potential prognostic significance in the prediction of LR in HCC. *AKR1C1* could be a promising therapeutic target for patients with LR-type liver cancer. Moreover, it is necessary to explore the molecular mechanism of LR and evaluate the therapeutic effect on these HCC patients.

Acknowledgments

Funding: This study was supported by grants from the National Natural Science Foundation of China (No. 81871927) and the Postgraduate Research & Practice Innovation Program of Jiangsu Province (No. KYCX20_2798).

Footnote

Reporting Checklist: The authors have completed the ARRIVE reporting checklist. Available at https://jgo.amegroups.com/article/view/10.21037/jgo-23-277/rc

Data Sharing Statement: Available at https://jgo.amegroups.com/article/view/10.21037/jgo-23-277/dss

Peer Review File: Available at https://jgo.amegroups.com/article/view/10.21037/jgo-23-277/prf

Conflicts of Interest: All authors have completed the ICMJE uniform disclosure form (available at https://jgo.amegroups.com/article/view/10.21037/jgo-23-277/coif). The authors have no conflicts of interest to declare.

Ethical Statement: The authors are accountable for all aspects of the work in ensuring that questions related to the accuracy or integrity of any part of the work are appropriately investigated and resolved. The study was conducted in accordance with the Declaration of Helsinki (as revised in 2013). Informed consent was obtained from the patients, and this research was approved by the Ethics Committee of Affiliated Hospital of Nantong University (No. 2018-L006). Animal experiments were performed under a project license (No. S20220228-004) granted by the Institute Ethics Committee at the Affiliated Hospital of Nantong University, in compliance with the guidance of the care and use of laboratory animals issued by the Ministry of Science and Technology of the China.

References

1. Chidambaranathan-Reghupaty S, Fisher PB, Sarkar D. Hepatocellular carcinoma (HCC): Epidemiology, etiology and molecular classification. Adv Cancer Res 2021;149:1-61.
2. Zhao Y, Zhang YN, Wang KT, et al. Lenvatinib for hepatocellular carcinoma: From preclinical mechanisms to anti-cancer therapy. Biochim Biophys Acta Rev Cancer 2020;1874:188391.
3. Komatsu S, Yano Y, Sofue K, et al. Assessment of lenvatinib treatment for unresectable hepatocellular carcinoma with liver cirrhosis. HPB (Oxford) 2020;22:1450-6.
4. Jin H, Shi Y, Lv Y, et al. EGFR activation limits the response of liver cancer to lenvatinib. Nature 2021;595:730-4.
5. Tang W, Chen Z, Zhang W, et al. The mechanisms of sorafenib resistance in hepatocellular carcinoma: theoretical basis and therapeutic aspects. Signal Transduct Target Ther 2020;5:87.
6. Ruf B, Heinrich B, Greten TF. Immunobiology and immunotherapy of HCC: spotlight on innate and innate-like immune cells. Cell Mol Immunol 2021;18:112-27.
7. Llovet JM, Zucman-Rossi J, Pikarsky E, et al. Hepatocellular carcinoma. Nat Rev Dis Primers 2016;2:16018.
8. Vogel A, Qin S, Kudo M, et al. Lenvatinib versus sorafenib for first-line treatment of unresectable hepatocellular carcinoma: patient-reported outcomes from a randomised, open-label, non-inferiority, phase 3 trial. Lancet

Gastroenterol Hepatol 2021;6:649-58.
9. Zeng CM, Chang LL, Ying MD, et al. Aldo-Keto Reductase AKR1C1-AKR1C4: Functions, Regulation, and Intervention for Anti-cancer Therapy. Front Pharmacol 2017;8:119.
10. Love MI, Huber W, Anders S. Moderated estimation of fold change and dispersion for RNA-seq data with DESeq2. Genome Biol 2014;15:550.
11. Smyth GK, Michaud J, Scott HS. Use of within-array replicate spots for assessing differential expression in microarray experiments. Bioinformatics 2005;21:2067-75.
12. Chin CH, Chen SH, Wu HH, et al. cytoHubba: identifying hub objects and sub-networks from complex interactome. BMC Syst Biol 2014;8 Suppl 4:S11.
13. Newman AM, Liu CL, Green MR, et al. Robust enumeration of cell subsets from tissue expression profiles. Nat Methods 2015;12:453-7.
14. Yu G, Wang LG, Han Y, et al. clusterProfiler: an R package for comparing biological themes among gene clusters. OMICS 2012;16:284-7.
15. Yang W, Soares J, Greninger P, et al. Genomics of Drug Sensitivity in Cancer (GDSC): a resource for therapeutic biomarker discovery in cancer cells. Nucleic Acids Res 2013;41:D955-61.
16. Li G, Du P, He J, et al. CircRNA circBACH1 (hsa_circ_0061395) serves as a miR-656-3p sponge to facilitate hepatocellular carcinoma progression through increasing SERBP1 expression. Biochem Biophys Res Commun 2021;556:1-8.
17. Li LM, Chen C, Ran RX, et al. Loss of TARBP2 Drives the Progression of Hepatocellular Carcinoma via miR-145-SERPINE1 Axis. Front Oncol 2021;11:620912.
18. Hou W, Bridgeman B, Malnassy G, et al. Integrin subunit beta 8 contributes to lenvatinib resistance in HCC. Hepatol Commun 2022;6:1786-802.
19. Hayes J, Peruzzi PP, Lawler S. MicroRNAs in cancer: biomarkers, functions and therapy. Trends Mol Med 2014;20:460-9.
20. Lee YS, Dutta A. MicroRNAs in cancer. Annu Rev Pathol 2009;4:199-227.
21. Zhao J, Zhu XC, Wu XS, et al. Identification of miR-4644 as a suitable endogenous normalizer for circulating miRNA quantification in hepatocellular carcinoma. J Cancer 2020;11:7032-44.
22. Al-Noshokaty TM, Mesbah NM, Abo-Elmatty DM, et al. Selenium nanoparticles overcomes sorafenib resistance in thioacetamide induced hepatocellular carcinoma in rats by modulation of mTOR, NF-κB pathways and LncRNA-AF085935/GPC3 axis. Life Sci 2022;303:120675.
23. Zhang Y, Luo M, Cui X, et al. Long noncoding RNA NEAT1 promotes ferroptosis by modulating the miR-362-3p/MIOX axis as a ceRNA. Cell Death Differ 2022;29:1850-63.
24. Tang K, Lv D, Miao L, et al. LncRNA TUG1 functions as a ceRNA for miR-1-3p to promote cell proliferation in hepatic carcinogenesis. J Clin Lab Anal 2022;36:e24415.
25. Zou Y, Sun Z, Sun S. LncRNA HCG18 contributes to the progression of hepatocellular carcinoma via miR-214-3p/CENPM axis. J Biochem 2020;168:535-46.
26. Tian Y, Liu H, Zhang C, et al. Comprehensive Analyses of Ferroptosis-Related Alterations and Their Prognostic Significance in Glioblastoma. Front Mol Biosci 2022;9:904098.
27. Miao YD, Kou ZY, Wang JT, et al. Prognostic implications of ferroptosis-associated gene signature in colon adenocarcinoma. World J Clin Cases 2021;9:8671-93.
28. Huang F, Zheng Y, Li X, et al. Ferroptosis-related gene AKR1C1 predicts the prognosis of non-small cell lung cancer. Cancer Cell Int 2021;21:567.
29. Zhang Z, Qiu X, Yan Y, et al. Evaluation of Ferroptosis-related Gene AKR1C1 as a Novel Biomarker Associated with the Immune Microenvironment and Prognosis in Breast Cancer. Int J Gen Med 2021;14:6189-200.
30. Hong Y, Lin M, Ou D, et al. A novel ferroptosis-related 12-gene signature predicts clinical prognosis and reveals immune relevancy in clear cell renal cell carcinoma. BMC Cancer 2021;21:831.
31. Chen S, Zhu JY, Zang X, et al. The Emerging Role of Ferroptosis in Liver Diseases. Front Cell Dev Biol 2021;9:801365.
32. Gao R, Kalathur RKR, Coto-Llerena M, et al. YAP/TAZ and ATF4 drive resistance to Sorafenib in hepatocellular carcinoma by preventing ferroptosis. EMBO Mol Med 2021;13:e14351.
33. Zhang X, Du L, Qiao Y, et al. Ferroptosis is governed by differential regulation of transcription in liver cancer. Redox Biol 2019;24:101211.
34. Faivre S, Rimassa L, Finn RS. Molecular therapies for HCC: Looking outside the box. J Hepatol 2020;72:342-52.
35. Forner A, Reig M, Bruix J. Hepatocellular carcinoma. Lancet 2018;391:1301-14.
36. Al-Salama ZT, Syed YY, Scott LJ. Lenvatinib: A Review in Hepatocellular Carcinoma. Drugs 2019;79:665-74.
37. Kanehisa M, Goto S. KEGG: kyoto encyclopedia of genes and genomes. Nucleic Acids Res 2000;28:27-30.
38. Yi C, Chen L, Lin Z, et al. Lenvatinib Targets FGF

Receptor 4 to Enhance Antitumor Immune Response of Anti-Programmed Cell Death-1 in HCC. Hepatology 2021;74:2544-60.
39. Chen B, Khodadoust MS, Liu CL, et al. Profiling Tumor Infiltrating Immune Cells with CIBERSORT. Methods Mol Biol 2018;1711:243-59.
40. Vilchez V, Turcios L, Marti F, et al. Targeting Wnt/β-catenin pathway in hepatocellular carcinoma treatment. World J Gastroenterol 2016;22:823-32.
41. Zhang Y, Zou J, Chen R. An M0 macrophage-related prognostic model for hepatocellular carcinoma. BMC Cancer 2022;22:791.
42. Huang L, Wang Z, Chang Y, et al. EFEMP2 indicates assembly of M0 macrophage and more malignant phenotypes of glioma. Aging (Albany NY) 2020;12:8397-412.
43. Zhang Z, Wang Z, Huang Y. Comprehensive Analyses of the Infiltrating Immune Cell Landscape and Its Clinical Significance in Hepatocellular Carcinoma. Int J Gen Med 2021;14:4695-704.
44. Zhang P, Sun H, Wen P, et al. circRNA circMED27 acts as a prognostic factor and mediator to promote lenvatinib resistance of hepatocellular carcinoma. Mol Ther Nucleic Acids 2022;27:293-303.
45. Chen GL, Ye T, Chen HL, et al. Xanthine dehydrogenase downregulation promotes TGFβ signaling and cancer stem cell-related gene expression in hepatocellular carcinoma. Oncogenesis 2017;6:e382.
46. Liu BHM, Tey SK, Mao X, et al. TPI1-reduced extracellular vesicles mediated by Rab20 downregulation promotes aerobic glycolysis to drive hepatocarcinogenesis. J Extracell Vesicles 2021;10:e12135.
47. Hou J, Wang L, Wu D. The root of Actinidia chinensis inhibits hepatocellular carcinomas cells through LAMB3. Cell Biol Toxicol 2018;34:321-32.
48. Chen J, Tang D, Li H, et al. Expression changes of serum LINC00941 and LINC00514 in HBV infection-related liver diseases and their potential application values. J Clin Lab Anal 2022;36:e24143.
49. Guan DX, Shi J, Zhang Y, et al. Sorafenib enriches epithelial cell adhesion molecule-positive tumor initiating cells and exacerbates a subtype of hepatocellular carcinoma through TSC2-AKT cascade. Hepatology 2015;62:1791-803.
50. Place RF, Li LC, Pookot D, et al. MicroRNA-373 induces expression of genes with complementary promoter sequences. Proc Natl Acad Sci U S A 2008;105:1608-13. Erratum in: Proc Natl Acad Sci U S A 2018;115:E3325.
51. Chen X, Kang R, Kroemer G, et al. Broadening horizons: the role of ferroptosis in cancer. Nat Rev Clin Oncol 2021;18:280-96.
52. Nie J, Lin B, Zhou M, et al. Role of ferroptosis in hepatocellular carcinoma. J Cancer Res Clin Oncol 2018;144:2329-37.
53. Kunimoto T, Nitta K, Tanaka T, et al. Antitumor activity of 7-ethyl-10-(4-(1-piperidino)-1-piperidino)carbonyloxy-camptothec in, a novel water-soluble derivative of camptothecin, against murine tumors. Cancer Res 1987;47:5944-7.
54. Xu L, Yuan-run Z, Jian C, et al. Anticancer effect of SN-38 combined with sorafenib on hepatocellular carcinoma in vitro and its mechanism. Zhejiang Da Xue Xue Bao Yi Xue Ban 2015;44:486-92.
55. Lu Y, Shen H, Huang W, et al. Genome-scale CRISPR-Cas9 knockout screening in hepatocellular carcinoma with lenvatinib resistance. Cell Death Discov 2021;7:359. Erratum in: Cell Death Discov 2022;8:74.

(English Language Editor: A. Kassem)

Cite this article as: Gao C, Chang L, Xu T, Li X, Chen Z. *AKR1C1* overexpression leads to lenvatinib resistance in hepatocellular carcinoma. J Gastrointest Oncol 2023;14(3):1412-1433. doi: 10.21037/jgo-23-277

Supplementary

Table S1 Significant KEGG pathways with adjusted P values <0.05 in AKR1C1

ID	Description	GeneRatio	BgRatio	pvalue	p.adjust	qvalue	geneID	Count
hsa04080	Neuroactive ligand-receptor interaction	35/307	362/8158	2.16E-07	1.16E-05	1.01E-05	6750/5644/2925/9248/552/6869/2690/2641/2695/3375/4986/1815/6863/3952/796/3352/1511/2568/6866/1392/1081/23620/2151/4544/7432/5539/9568/1144/1136/3357/51052/7200/4295/2797/1134	35
hsa05207	Chemical carcinogenesis - receptor activation	21/307	212/8158	4.52E-05	0.00120767	0.001052218	54578/4609/114/2247/107/7363/54577/2253/54657/2949/688/1950/1545/1543/54600/7471/1136/8822/54575/6258/1576	21
hsa04020	Calcium signaling pathway	20/307	240/8158	0.000694927	0.01159659	0.010103869	444/810/2925/114/552/6869/2247/9965/107/5350/2253/4915/1950/2263/10345/57172/8822/3357/8911/55283	20
hsa04976	Bile secretion	18/307	89/8158	3.75E-09	5.00E-07	4.36E-07	1244/54578/477/114/107/9429/7363/54577/54657/3781/10864/366/54600/6523/9376/343/54575/1576	18
hsa05226	Gastric cancer	17/307	149/8158	4.14E-05	0.00120767	0.001052218	8313/7475/83998/4609/2247/9965/6932/51176/2253/1496/1950/2263/399694/7471/8822/6258/7476	17
hsa04310	Wnt signaling pathway	17/307	170/8158	0.000214756	0.00477832	0.004163251	8313/7475/85407/84870/4609/6932/54894/147111/51176/59352/27121/7471/8549/1501/340419/7476/50964	17
hsa00140	Steroid hormone biosynthesis	16/307	61/8158	4.80E-10	1.28E-07	1.12E-07	1645/1646/54578/1585/3283/7363/54577/6820/54657/3284/1545/1543/54600/1551/54575/1576	16
hsa00980	Metabolism of xenobiotics by cytochrome P450	15/307	78/8158	1.56E-07	1.16E-05	1.01E-05	1645/218/54578/7363/54577/222/54657/2949/1545/1543/1553/54600/1549/54575/1576	15
hsa05204	Chemical carcinogenesis - DNA adducts	14/307	69/8158	2.03E-07	1.16E-05	1.01E-05	1646/54578/7363/54577/54657/2949/1545/1543/1553/54600/1551/1549/54575/1576	14
hsa04974	Protein digestion and absorption	14/307	103/8158	2.84E-05	0.000947345	0.000825402	1357/1358/5644/440387/477/1504/10136/23436/4311/1360/1294/340024/1359/1280	14
hsa04934	Cushing syndrome	14/307	155/8158	0.00205844	0.024981974	0.021766278	8313/7475/114/3283/6932/107/51176/3284/1392/7471/6770/3776/8911/7476	14
hsa04972	Pancreatic secretion	13/307	102/8158	0.000107898	0.00261898	0.002281863	1357/1358/5644/440387/477/114/1504/10136/107/23436/1360/1359/1179	13
hsa05224	Breast cancer	13/307	147/8158	0.003534695	0.036297937	0.031625642	8313/7475/4609/2247/9965/6932/51176/2253/1950/399694/7471/8822/7476	13
hsa00830	Retinol metabolism	12/307	68/8158	7.14E-06	0.000317619	0.000276735	216/54578/7363/54577/54657/1543/54600/1551/195814/1549/54575/1576	12
hsa00982	Drug metabolism - cytochrome P450	12/307	72/8158	1.32E-05	0.000501826	0.00043723	218/54578/7363/54577/222/2326/54657/2949/54600/1549/54575/1576	12
hsa03320	PPAR signaling pathway	10/307	75/8158	0.000464845	0.008865257	0.007724115	729359/2173/2170/23305/4312/2172/9370/23205/4973/6258	10
hsa00983	Drug metabolism - other enzymes	10/307	80/8158	0.00078221	0.011602781	0.010109263	54578/1066/7363/54577/54657/2949/54600/1549/54575/1576	10
hsa04911	Insulin secretion	10/307	86/8158	0.001379095	0.017534212	0.015277196	477/114/2645/2641/107/2695/3781/157855/6833/3651	10
hsa04925	Aldosterone synthesis and secretion	10/307	98/8158	0.003670578	0.036297937	0.031625642	810/477/1585/114/3283/107/3284/57172/6770/8911	10
hsa04913	Ovarian steroidogenesis	8/307	51/8158	0.000569401	0.010135333	0.008830706	114/3283/107/3284/1545/1081/1543/6770	8
hsa05217	Basal cell carcinoma	8/307	63/8158	0.002343701	0.027207307	0.023705164	8313/7475/6932/51176/652/2736/7471/7476	8
hsa04929	GnRH secretion	8/307	64/8158	0.002593024	0.028847388	0.025134132	6696/3760/3781/1081/610/9568/2797/8911	8
hsa04927	Cortisol synthesis and secretion	8/307	65/8158	0.002862624	0.030572824	0.026637469	114/3283/107/3284/190/6770/3776/8911	8
hsa00040	Pentose and glucuronate interconversions	7/307	35/8158	0.000270481	0.005555255	0.004840179	57016/54578/7363/54577/54657/54600/54575	7
hsa00860	Porphyrin metabolism	7/307	43/8158	0.001001493	0.014073606	0.012262042	54578/7363/54577/54657/54600/212/54575	7
hsa00053	Ascorbate and aldarate metabolism	6/307	30/8158	0.000747435	0.011602781	0.010109263	54578/7363/54577/54657/54600/54575	6
hsa00340	Histidine metabolism	5/307	22/8158	0.001134205	0.015141641	0.013192599	218/84735/222/57571/131669	5

KEGG, Kyoto Encyclopedia of Genes and Genomes.

https://dx.doi.org/10.21037/jgo-23-277

Table S2 Significant KEGG pathways with adjusted P values <0.05 in SERPINE1

ID	Description	GeneRatio	BgRatio	pvalue	p.adjust	qvalue	geneID	Count
hsa04080	Neuroactive ligand-receptor interaction	39/312	362/8158	3.10E-09	4.17E-07	3.45E-07	4922/5021/6750/1134/5644/2641/2797/9248/2357/3952/4986/6344/2555/6863/2568/8484/799/796/1136/2925/1815/6866/7432/2692/6869/4295/130576/5030/1392/3352/3375/4544/2695/51052/186/1511/7200/1144/51083	39
hsa04151	PI3K-Akt signaling pathway	31/312	354/8158	1.24E-05	0.000476417	0.000393364	3371/9965/1293/2253/1278/1311/1277/2260/7057/3675/3918/5008/3694/1441/5156/3691/2056/3696/3381/7058/3909/3082/90993/3569/2248/26291/26281/8822/8074/8115/2786	31
hsa05165	Human papillomavirus infection	25/312	331/8158	0.000855304	0.010458031	0.008634884	11317/3371/1293/1278/1311/1277/7057/3675/3918/5315/3694/3691/5743/3696/7475/3381/7058/3909/7472/90993/80326/8313/7482/7471/7476	25
hsa04060	Cytokine-cytokine receptor interaction	24/312	295/8158	0.000374819	0.005979127	0.004936786	3589/3576/3976/6347/3952/5008/1441/3596/2056/10344/6374/3623/9547/3598/9966/2921/2658/53832/3569/6354/970/2919/6370/10563	24
hsa04974	Protein digestion and absorption	22/312	103/8158	2.88E-11	7.74E-09	6.39E-09	1357/1301/5644/1293/1296/1281/1278/477/1358/1289/1277/1307/1300/3783/4311/1302/440387/1504/1308/10136/169044/7512	22
hsa04310	Wnt signaling pathway	21/312	170/8158	1.84E-06	9.91E-05	8.18E-05	8061/6422/6423/7475/6424/4920/147111/7472/80326/85407/27121/8313/6425/4316/164284/7482/7471/340419/7476/11197/50964	21
hsa05205	Proteoglycans in cancer	20/312	205/8158	0.000106304	0.002859573	0.002361064	5329/5328/1278/1277/2260/7057/3710/4313/7475/4318/7291/3082/7472/4060/1634/80326/7482/7471/117581/7476	20
hsa04510	Focal adhesion	19/312	201/8158	0.000238566	0.004936486	0.004075909	3371/1293/1278/1311/1277/7057/3675/3918/3694/5156/3691/10398/3696/3381/7058/3909/3082/5923/4633	19
hsa04657	IL-17 signaling pathway	18/312	94/8158	1.21E-08	1.08E-06	8.95E-07	6279/6280/3576/2354/4312/8061/2353/6347/3596/5743/6374/4318/2921/3569/4322/6354/2919/4586	18
hsa04024	cAMP signaling pathway	18/312	221/8158	0.001976168	0.020910041	0.017264796	5021/6750/2641/477/2353/10398/810/338442/90993/8843/2867/7432/1080/1392/3352/2695/84152/114	18
hsa04020	Calcium signaling pathway	18/312	240/8158	0.004793581	0.037925686	0.031314106	5021/9965/2253/2260/3710/5156/810/3082/8911/2925/2248/26291/26281/6869/8822/8074/114/57172	18
hsa04915	Estrogen signaling pathway	17/312	138/8158	1.86E-05	0.000626775	0.00051751	54474/3859/3872/2353/3710/810/4313/4318/90993/3310/7031/25984/114/3880/3860/3868/3861	17
hsa05226	Gastric cancer	17/312	149/8158	5.07E-05	0.00151577	0.001251526	9965/2253/7475/1496/3082/7472/80326/2248/26291/8313/26281/8822/7482/7471/83998/8074/7476	17
hsa05207	Chemical carcinogenesis - receptor activation	17/312	212/8158	0.00307574	0.027579134	0.022771267	9314/2253/2353/1545/688/90993/1136/54577/2248/26281/8822/2940/7471/7367/114/2944/54575	17
hsa04972	Pancreatic secretion	16/312	102/8158	1.37E-06	9.21E-05	7.60E-05	1357/5644/477/1358/3710/6344/5874/30814/1080/440387/1504/1811/1179/10136/114/5406	16
hsa05224	Breast cancer	16/312	147/8158	0.000147882	0.003338944	0.002756867	9965/2253/2353/2260/7475/7472/80326/2248/26291/8313/26281/8822/7482/7471/8074/7476	16
hsa04512	ECM-receptor interaction	14/312	88/8158	5.33E-06	0.000238804	0.000197174	3371/1293/1278/1311/1277/7057/3675/3918/3694/3691/3696/3381/7058/3909	14
hsa04550	Signaling pathways regulating pluripotency of stem cells	13/312	143/8158	0.003195141	0.027725579	0.022892182	3976/9314/2260/7475/7472/10637/80326/8313/7482/7471/7044/3231/7476	13
hsa04934	Cushing syndrome	13/312	155/8158	0.006333007	0.048673681	0.040188404	3710/7475/7472/90993/8911/80326/8313/1392/7482/6770/7471/7476/114	13
hsa05410	Hypertrophic cardiomyopathy	12/312	90/8158	0.000148949	0.003338944	0.002756867	1674/3675/3694/3691/3696/3569/4634/786/70/55799/4633/59284	12
hsa05150	Staphylococcus aureus infection	12/312	96/8158	0.000276714	0.004962403	0.004097308	54474/3383/1670/3859/3872/2357/25984/1668/3880/3860/3868/3861	12
hsa05414	Dilated cardiomyopathy	12/312	96/8158	0.000276714	0.004962403	0.004097308	1674/3675/3694/3691/3696/4634/786/70/55799/4633/59284/114	12
hsa04061	Viral protein interaction with cytokine and cytokine receptor	12/312	100/8158	0.000405908	0.006066067	0.00500857	3576/6347/10344/6374/9547/2921/53832/3569/6354/2919/6370/10563	12
hsa05146	Amoebiasis	12/312	102/8158	0.000487615	0.006903601	0.005700097	3576/1281/1278/1277/3918/3909/2921/3569/6317/2919/1511/6318	12
hsa04668	TNF signaling pathway	12/312	112/8158	0.001133823	0.013260799	0.010949045	3383/3976/9021/2353/6347/5743/6374/4318/2921/90993/3569/2919	12
hsa04928	Parathyroid hormone synthesis, secretion and action	11/312	106/8158	0.002335206	0.02326557	0.019209686	5744/2353/2260/3710/860/90993/4322/8074/114/10568/50964	11
hsa05218	Melanoma	10/312	72/8158	0.000377863	0.005979127	0.004936786	9965/2253/2260/5156/3082/2248/26291/26281/8822/8074	10
hsa05412	Arrhythmogenic right ventricular cardiomyopathy	10/312	77/8158	0.000652995	0.00836455	0.006906359	1674/3675/3694/3691/3696/1496/88/786/55799/59284	10
hsa04976	Bile secretion	10/312	89/8158	0.002021045	0.020910041	0.017264796	477/358/6523/6344/54577/1080/7367/114/54575/9376	10
hsa05323	Rheumatoid arthritis	10/312	93/8158	0.002807684	0.026043688	0.021503495	3589/3383/3576/4312/2353/6347/6374/2921/3569/2919	10
hsa04933	AGE-RAGE signaling pathway in diabetic complications	10/312	100/8158	0.004757981	0.037925686	0.031314106	5054/3383/3576/2152/1281/1278/1277/6347/4313/3569	10
hsa05144	Malaria	8/312	50/8158	0.000552286	0.007428244	0.006133279	3383/3576/1311/6347/7057/7058/3082/3569	8
hsa05217	Basal cell carcinoma	8/312	63/8158	0.00259144	0.024896336	0.020556161	7475/7472/80326/8313/7482/7471/2736/7476	8
hsa04614	Renin-angiotensin system	5/312	23/8158	0.001510025	0.016924869	0.013974358	1215/4311/5972/186/1511	5
hsa00910	Nitrogen metabolism	4/312	17/8158	0.003364015	0.028278749	0.023348919	759/1373/768/761	4

KEGG, Kyoto Encyclopedia of Genes and Genomes.

https://dx.doi.org/10.21037/jgo-23-277

Table S3 The data of 80 significant abnormally expressed genes from RNA-seq

Gene ID	High expression genes	Gene ID	Low expression genes
ENSG00000215912	*TTC34*	ENSG00000215274	*GAGE10*
ENSG00000261915	*AC026954.2*	ENSG00000187689	*AMTN*
ENSG00000186529	*CYP4F3*	ENSG00000138100	*TRIM54*
ENSG00000141574	*SECTM1*	ENSG00000175294	*CATSPER1*
ENSG00000115041	*KCNIP3*	ENSG00000139211	*AMIGO2*
ENSG00000100867	*DHRS2*	ENSG00000171564	*FGB*
ENSG00000168481	*LGI3*	ENSG00000134516	*DOCK2*
ENSG00000089820	*ARHGAP4*	ENSG00000176020	*AMIGO3*
ENSG00000240065	*PSMB9*	ENSG00000182578	*CSF1R*
ENSG00000168874	*ATOH8*	ENSG00000179546	*HTR1D*
ENSG00000187134	*AKR1C1*	ENSG00000171560	*FGA*
ENSG00000271447	*MMP28*	ENSG00000122861	*PLAU*
ENSG00000128165	*ADM2*	ENSG00000135919	*SERPINE2*
ENSG00000171798	*KNDC1*	ENSG00000243137	*PSG4*
ENSG00000140961	*OSGIN1*	ENSG00000039068	*CDH1*
ENSG00000197063	*MAFG*	ENSG00000183128	*CALHM3*
ENSG00000119227	*PIGZ*	ENSG00000101076	*HNF4A*
ENSG00000197119	*SLC25A29*	ENSG00000138207	*RBP4*
ENSG00000184451	*CCR10*	ENSG00000101680	*LAMA1*
ENSG00000203618	*GP1BB*	ENSG00000175874	*CREG2*
ENSG00000163794	*UCN*	ENSG00000105825	*TFPI2*
ENSG00000188747	*NOXA1*	ENSG00000198959	*TGM2*
ENSG00000137070	*IL11RA*	ENSG00000130477	*UNC13A*
ENSG00000175040	*CHST2*	ENSG00000128510	*CPA4*
ENSG00000181264	*TLCD5*	ENSG00000073910	*FRY*
ENSG00000049769	*PPP1R3F*	ENSG00000141968	*VAV1*
ENSG00000138622	*HCN4*	ENSG00000172985	*SH3RF3*
ENSG00000151632	*AKR1C2*	ENSG00000150551	*LYPD1*
ENSG00000184371	*CSF1*	ENSG00000226887	*ERVMER34-1*
ENSG00000006047	*YBX2*	ENSG00000100302	*RASD2*
ENSG00000161921	*CXCL16*	ENSG00000164687	*FABP5*
ENSG00000162591	*MEGF6*	ENSG00000122547	*EEPD1*
ENSG00000165475	*CRYL1*	ENSG00000120708	*TGFBI*
ENSG00000126091	*ST3GAL3*	ENSG00000143515	*ATP8B2*
ENSG00000175318	*GRAMD2A*	ENSG00000120162	*MOB3B*
ENSG00000182685	*BRICD5*	ENSG00000187720	*THSD4*
ENSG00000144152	*FBLN7*	ENSG00000215182	*MUC5AC*
ENSG00000162545	*CAMK2N1*	ENSG00000124225	*PMEPA1*
		ENSG00000162745	*OLFML2B*
		ENSG00000198805	*PNP*
		ENSG00000127920	*GNG11*
		ENSG00000106366	*SERPINE1*

https://dx.doi.org/10.21037/jgo-23-277

Table S4 MiRNA prediction data

miDIP	starBase
hsa-miR-197-3p	hsa-miR-634
hsa-miR-135a-5p	hsa-miR-1226-3p
hsa-miR-145-5p	hsa-miR-4644
hsa-miR-185-5p	hsa-miR-5701
hsa-miR-365a-3p	hsa-miR-3190-5p
hsa-miR-135b-5p	hsa-miR-597-5p
hsa-miR-324-3p	hsa-miR-3137
hsa-miR-338-3p	hsa-miR-6830-3p
hsa-miR-556-5p	hsa-miR-6165
hsa-miR-628-5p	hsa-miR-5196-3p
hsa-miR-944	hsa-miR-6717-5p
hsa-miR-1286	hsa-miR-1251-3p
hsa-miR-1913	hsa-miR-1537-3p
hsa-miR-4306	hsa-miR-320a-5p
hsa-miR-3918	hsa-miR-6790-3p
hsa-miR-4644	hsa-miR-11399
hsa-miR-4731-5p	hsa-miR-10399-3p
hsa-miR-506-5p	

https://dx.doi.org/10.21037/jgo-23-277